

# Materials- Sutton

Tomás Ricardo Basile Álvarez  
316617194

July 21, 2021

## Introduction

### State Equation

In a fluid or gas, the equation of state relates the pressure to the volume and temperature of a material. In the solid state, the full stress and strain tensors replace the thermodynamic variables pressure and volume.

For example, for small elastic strains, Hooke's law relates the strain and the stress.

We introduce the **Wigner Seitz radius**  $r_{ws}$  as the radius of a sphere whose volume equals the volume per atom in the material, thus, if there are  $N$  atoms per unit volume:

$$N \frac{4\pi}{3} r_{ws}^3 = 1$$

**Binding energy:** Is the total energy of the metal relative to the energy of the same number of isolated atoms. It tends to zero as the atoms are infinitely separated, and it has a minimum, negative value at the equilibrium value of  $r_{ws} = r_{ws}^e$ . The binding energy at the minimum is  $E_b^e$ .

Different materials have different equilibrium values and binding energy curves.

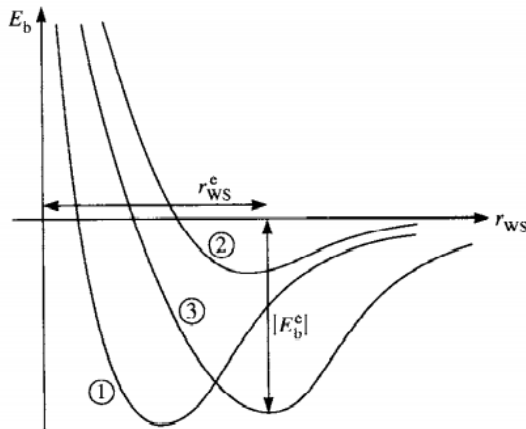


**Fig. 1.1** The binding energy,  $E_b$ , as a function of the Wigner–Seitz radius,  $r_{ws}$ , for three metals. The minimum of each binding energy curve occurs at  $r_{ws} = r_{ws}^e$  and  $E_b = -|E_b^e|$ .

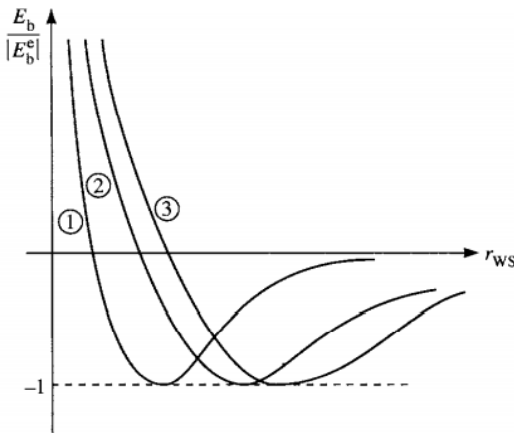
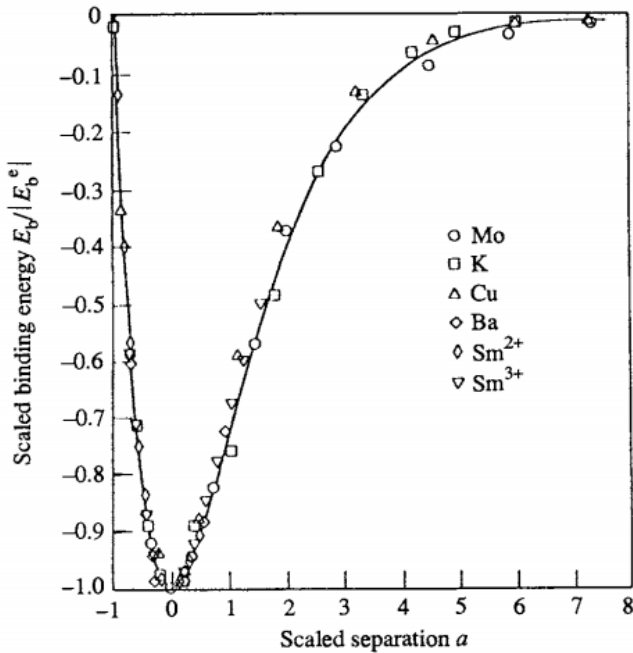


**Fig. 1.2** The scaled binding energy,  $E_b/|E_b^e|$ , as a function of the Wigner–Seitz radius,  $r_{ws}$ , for the same three metals as in Fig. 1.1. The minima occur at  $E_b/|E_b^e| = -1$ , but different values of  $r_{ws}$ .

We can even scale the length as  $a = (r_{ws} - r_{ws}^e)/l$  where  $l = \left( \frac{|E_b^e|}{E_b''(r_{ws}^e)} \right)^{1/2}$ . Then, we find a 'universal' equation of state for metals.

---

### The 'universal' equation of state for metals 5



## The Hydrogen Atom

We first recall that each quantum state of the hydrogen atom is labelled by four quantum numbers:

- $n = 1, 2, 3, \dots$ : The principal quantum number. The energy of the state is proportional to  $1/n^2$
- $l = 0, 1, 2, \dots, n-1$  the angular momentum number. The total angular momentum is given by  $\sqrt{l(l+1)}\hbar$
- $m = -l, -l+1, \dots, l-1, l$  is the magnetic quantum number. It gives the component of angular momentum vector in the z-axis. The angular momentum in this direction is  $m\hbar$
- $m_s$  is the electron spin and is  $1/2$  or  $-1/2$  corresponding to spin up or down.

We shall say that each  $|n, l, m\rangle$  state is occupied by two electrons (one of each spin).

The wave function are:

$$\Psi_{nlm}(r, \theta, \phi) = R_{nl}(r)Y_{lm}(\theta, \phi)$$

The solutions are orthogonal:

$$\int \psi_{nlm}^* \psi_{n'l'm'} d\vec{r} = \delta_{nn'} \delta_{mm'} \delta_{ll'}$$

If two electrons have the same  $l$  and  $m$ , then they must satisfy:

$$\int_0^\infty R_{nl}(r)R_{n'l}(r)r^2 dr = \delta_{nn'}$$

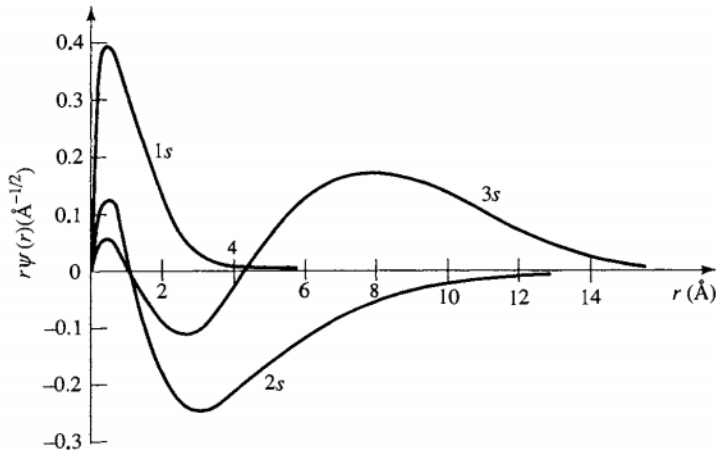


**Fig. 1.7** The three s states of lowest energy for atomic hydrogen. The orbitals, multiplied by  $r$ , are plotted as a function of distance,  $r$ , from the nucleus. From Harrison (1980).

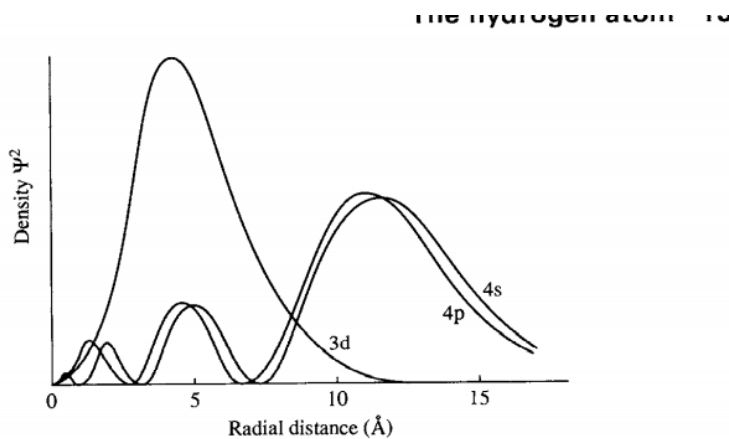


**Fig. 1.8** The densities of 3d, 4s, and 4p orbitals in hydrogen as a function of radial distance. (After Harrison 1980)

## P-Orbitals

For p orbitals, the atomic orbitals are:

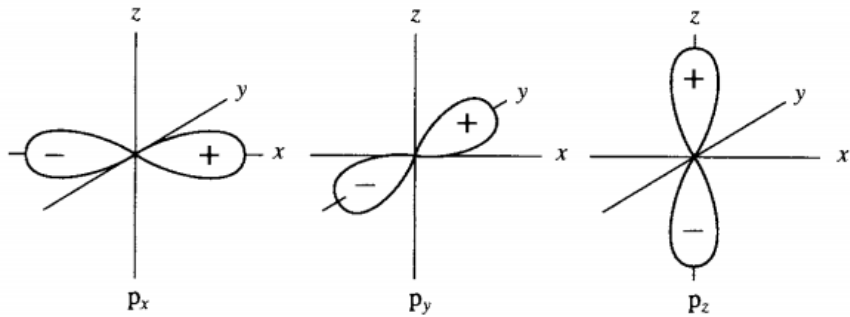


**Fig. 1.10**  $p_x$ ,  $p_y$ , and  $p_z$  atomic orbitals.

### d orbitals

And for  $d$  orbitals, they are:

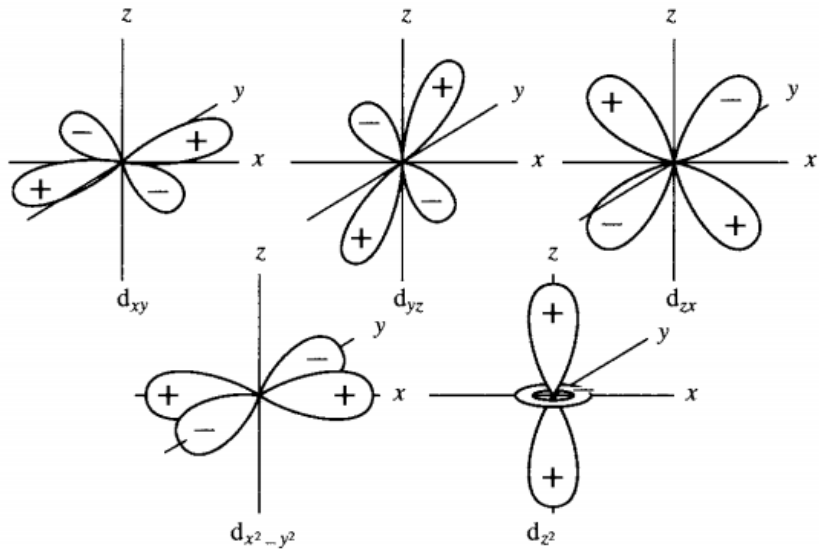


**Fig. 1.11**  $d_{xy}$ ,  $d_{yz}$ ,  $d_{zx}$ ,  $d_{x^2-y^2}$ , and  $d_{z^2}$  atomic orbitals.

The angular character of the  $d$  orbitals is important.

Moving to the other elements of the periodic table, we recall that the degeneracy of states with same principal quantum number but different angular momenta is lifted by the presence of electron-electron interactions. But still, it is possible to think of each electron as moving independently. We say that each electron moves in the field of the nucleus and the other electrons.

The usual order of energies in a given atom is:

$$1s < 2s < 2p < 3s < 3p < 3d \sim 4s \dots$$

---

The reason why the energies in any given  $n$  shell increase in the order  $ns, np, nd, nf$  is easy to see. The increasing number of planar nodes in these orbitals (0,1,2,3 respectively) forces the electron to spend an increasing amount of time further from the nucleus, where the attractive electrostatic field of the nucleus is screened by the other electrons.

The electron configurations are then determined by the aufbau principle, the lowest available states are filled subject to the exclusion principle, which asserts that no orbital may contain more than two electrons.

The chemical behavior of elements is determined by the outermost electron shell. A +1 valency in alkali metals means that the atom has a last electron easily removed (it is the only one in the last shell).

**Table 1.2** The electron configurations of the first 36 elements

Z	Element	Electron configuration									
		1s	2s	2p	3s	3p	3d	4s	4p	4d	4f
1	H <i>hydrogen</i>	1									
2	He <i>helium</i>	2									
3	Li <i>lithium</i>			1							
4	Be <i>beryllium</i>			2							
5	B <i>boron</i>			2	1						
6	C <i>carbon</i>	Filled		2	2						
7	N <i>nitrogen</i>	(2)		2	3						
8	O <i>oxygen</i>			2	4						
9	F <i>fluorine</i>			2	5						
10	Ne <i>neon</i>			2	6						
11	Na <i>sodium</i>					1					
12	Mg <i>magnesium</i>					2					
13	Al <i>aluminium</i>					2	1				
14	Si <i>silicon</i>	Filled				2	2				
15	P <i>phosphorus</i>					2	3				
16	S <i>sulfur</i>					2	4				
17	Cl <i>chlorine</i>					2	5				
18	A <i>argon</i>					2	6				
19	K <i>potassium</i>									1	
20	Ca <i>calcium</i>									2	
21	Sc <i>scandium</i>							1		2	
22	Ti <i>titanium</i>							2		2	
23	V <i>vanadium</i>	Filled						3		2	
24	Cr <i>chromium</i>								5	1	
25	Mn <i>manganese</i>	(2)		(8)					5	2	
26	Fe <i>iron</i>								6	2	
27	Co <i>cobalt</i>								7	2	
28	Ni <i>nickel</i>								8	2	
29	Cu <i>copper</i>								10	1	
30	Zn <i>zinc</i>								10	2	
31	Ga <i>gallium</i>									2	1
32	Ge <i>germanium</i>	Filled								2	2
33	As <i>arsenic</i>									2	3
34	Se <i>selenium</i>	(2)		(8)			(18)			2	4
35	Br <i>bromine</i>									2	5
36	Kr <i>krypton</i>									2	6

Number of electrons  
in each state

## The Diatomic Molecule

### Review of Bras, kets.

#### Vectors

A vector is something with magnitude and direction. To say the direction, we need to agree

---

on a coordinate basis. We agree on a orthogonal basis  $\vec{e}_1, \vec{e}_2, \vec{e}_3$ . Then the vector  $\vec{v}$  is:

$$\vec{v} = (\vec{v} \cdot \vec{e}_1)\vec{e}_1 + (\vec{v} \cdot \vec{e}_2)\vec{e}_2 + (\vec{v} \cdot \vec{e}_3)\vec{e}_3$$

Now, consider a quantum state  $|\Psi\rangle$  in real space. At each point  $\vec{r}$ , the quantum state is represented by the function  $\Psi(\vec{r})$ . The quantum state could be expanded in a set of orthonormal basis states  $\{|\phi\rangle\}$  as:

$$|\Psi\rangle = \sum_{all\phi} |\phi\rangle \langle \phi| \Psi\rangle$$

The expansion coefficients are the  $\langle \phi | \Psi \rangle$ , which are simply numbers. We call  $|\Psi\rangle$  the state vector and  $\langle \phi | \Psi \rangle$  the components in the basis set  $\{|\phi\rangle\}$ .

There is an important distinction between a state vector  $|\Psi\rangle$  and its representation in some basis.

Since  $|\Psi\rangle$  appears on both sides, it follows that:

$$\sum_{all\phi} |\phi\rangle \langle \phi| = I$$

This is the condition for an orthonormal complete basis.

The dot product is defined as:

$$\langle \Psi | \chi \rangle = \int_{all\ space} \Psi^*(r) \chi(r) dr$$

If  $|\Psi\rangle$  and  $|\chi\rangle$  are two different state vectors, the overlap between them is calculated as:

$$\langle \Psi | \chi \rangle = \langle \Psi | I | \chi \rangle = \langle \Psi | \sum_{all\phi} |\phi\rangle \langle \phi| \chi \rangle = \sum_{all\phi} \langle \Psi | \phi \rangle \langle \phi | \chi \rangle$$

A possibly more familiar expression for this overlap is in terms of the wave functions  $\Psi(\vec{r}), \chi(\vec{r})$ , in which case:

$$\langle \Psi | \chi \rangle = \int_{all\space} \Psi^*(\vec{r}) \chi(\vec{r}) dr = \int_{all\space} \langle \Psi | \vec{r} \rangle \langle \vec{r} | \chi \rangle dr$$

The sum over the basis vectors  $|\phi\rangle$  is replaced with an integral because we are using the continuous variable  $\vec{r}$ . The analogue of the identity operator in this case would be:

$$I = \int_{all\space} |\vec{r}\rangle \langle \vec{r}| dr$$

---

Suppose we have two sets of basis states  $\{|\phi\rangle\}$  and  $\{|i\rangle\}$  such that they span the same Hilbert space. We can represent a state  $|\Psi\rangle$  in this space using either basis:

$$|\Psi\rangle = \sum_{all\phi} |\phi\rangle\langle\phi|\Psi\rangle$$

$$|\Psi\rangle = \sum_{alli} |i\rangle\langle i|\Psi\rangle$$

Where, because they are basis, we have  $I = \sum|\phi\rangle\langle\phi|$  and  $I = \sum|i\rangle\langle i|$ . We can even find a relation between the coefficients in both bases:

$$\langle\phi|\Psi\rangle = \langle\phi|I|\Psi\rangle = \sum_i \langle\phi|i\rangle\langle i|\Psi\rangle$$

### Operator:

Suppose we have an operator  $L$  such that  $|\chi\rangle = L|\Psi\rangle$

If we use a basis  $\{|i\rangle\}$  to represent the state vectors. The coefficient  $\langle j|\chi\rangle$  of  $|\chi\rangle$  in this basis is given by:

$$\langle j|\chi\rangle = \langle j|L|\Psi\rangle$$

Where  $|j\rangle$  is one of the basis states. We can write it as:

$$\langle j|\chi\rangle = \langle j|L|\Psi\rangle = \langle j|L| \sum_{all\ i} |i\rangle\langle i||\Psi\rangle = \sum_{all\ i} \langle j|L|i\rangle\langle i|\Psi\rangle$$

vector  $\xi$  is related to the vector  $\Psi$  by a matrix  $L$

$$\begin{pmatrix} \xi_1 \\ \xi_2 \\ \xi_3 \end{pmatrix} = \begin{pmatrix} L_{11} & L_{12} & L_{13} \\ L_{21} & L_{22} & L_{23} \\ L_{31} & L_{32} & L_{33} \end{pmatrix} \begin{pmatrix} \Psi_1 \\ \Psi_2 \\ \Psi_3 \end{pmatrix} \quad (2.13)$$

or in component form

$$\xi_j = \sum_{i=1}^3 L_{ji} \Psi_i. \quad (2.14)$$

Comparing this equation with eqn (2.12) we see that the quantities  $\langle j|L|i\rangle$  and  $L_{ji}$  serve the same role. For this reason  $\langle j|L|i\rangle$  is called a matrix element of the operator  $L$ .

Then, in general we have:

$$|\chi\rangle = \sum_{all\ i} |i\rangle\langle i|L| \sum_{all\ j} |j\rangle\langle j||\Psi\rangle = \sum_{all\ i} \sum_{all\ j} |i\rangle\langle i|L|i\rangle\langle i|\Psi\rangle$$

Then, we find that:

$$L = \sum_{all\ i} \sum_{all\ j} |i\rangle\langle i|L|i\rangle\langle i|$$

---

## A Homonuclear diatomic Molecule

Consider the  $H_2$  molecule in its ground state. If we attempted to solve the Schrodinger equation, the e-e interaction would make it too difficult. Instead we shall follow a simple molecular orbital approach and obtain a qualitative picture.

Let  $|1\rangle$  denote the electron state on the first atom and  $|2\rangle$  that on the second atom. Since we are interested in the ground state, we shall assume that  $|1\rangle$  and  $|2\rangle$  are the ground state 1s, and let the energy of the electron in these states be  $E_f$ :

$$H_1|1\rangle = E_f|1\rangle \quad , \quad H_2|2\rangle = E_f|2\rangle$$

Where  $H_1, H_2$  are the Hamiltonians for the isolated atoms 1 and 2. We now assume that the two basis states form an adequate basis in which to expand the ground state  $|\Psi\rangle$  of the whole molecule:

$$|\Psi\rangle = c_1|1\rangle + c_2|2\rangle$$

And we assume that these basis vectors are orthonormal.  $\langle 1|2\rangle = \langle 2|1\rangle = 0$  and  $\langle 1|1\rangle = \langle 2|2\rangle = 1$ . This assumption breaks down when we bring the atoms together and the 1s orbitals start to overlap, but we will use this approximation and still get some useful info.

Therefore, the coefficients of the expansion of  $|\Psi\rangle$  in terms of the states are  $c_1 = \langle 1|\Psi\rangle$  and  $c_2 = \langle 2|\Psi\rangle$ .

The Schrodinger equation for the molecular state is:

$$H|\Psi\rangle = E|\Psi\rangle$$

Or substituting, we have:

$$H(c_1|1\rangle + c_2|2\rangle) = E(c_1|1\rangle + c_2|2\rangle)$$

We project the equation into the basis states:

$$\begin{aligned} \langle 1|H(c_1|1\rangle + c_2|2\rangle) &= \langle 1|E(c_1|1\rangle + c_2|2\rangle) \\ \langle 2|H(c_1|1\rangle + c_2|2\rangle) &= \langle 2|E(c_1|1\rangle + c_2|2\rangle) \end{aligned}$$

This gives the equations:

$$E_0c_1 + H_{12}c_2 = Ec_1$$

$$H_{21}c_1 + E_0c_2 = Ec_2$$

Where  $\langle i|H|j\rangle = H_{ij}$  and we used orthonormality of the basis. And  $H_{11} = H_{22} = E_0$  (These values are just the energies of a single H atom (expected value of  $H$  in state  $|1\rangle$  and  $|2\rangle$ )).

Then, for non trivial solutions, we need a non zero determinant, that is:

$$\left| \begin{pmatrix} E_0 - E & H_{12} \\ H_{21} & E_0 - E \end{pmatrix} \right| = 0$$

Expanding the determinant, we get:

$$E^2 - 2E_0E + E_0^2 - H_{21}H_{12} = 0$$

Since  $H$  is hermitian,  $H_{12} = H_{21}^*$ . But we have assumed real atomic orbitals (1s orbitals, not complex) for the basis. So they are a real number,  $H_{12} = H_{21} \equiv \beta$ . The solutions are:

$E_b = E_0 + \beta$
$E_a = E_0 - \beta$

The normalized stationary state vector with eigenvalue  $E_b$  is:

$$|\Psi_b\rangle = \frac{1}{\sqrt{2}}(|1\rangle + |2\rangle)$$

(We can see that it satisfies the equation  $H|\Psi_b\rangle = E_b|\Psi_b\rangle$ )

And that of  $E_a$  is:

$$|\Psi_a\rangle = \frac{1}{\sqrt{2}}(|1\rangle - |2\rangle)$$

(We can see that it satisfies the equation  $H|\Psi_a\rangle = E_a|\Psi_a\rangle$ )

So we have found two states, one with energy  $E_0 + \beta$  and one with  $E_0 - \beta$ .

What is the sign of  $\beta$ ? To answer this, let us assume that the Hamiltonian operator is of the form  $H = -\frac{\hbar^2}{8\pi^2m}\nabla^2 + V_1(\vec{r}) + V_2(\vec{r})$ .

Where  $V_1(\vec{r})$  is the potential of the first nucleus and  $V_2(\vec{r})$  of the second and we are ignoring the electron-electron interaction.

Therefore, we have that:

$$\begin{aligned} H_{12} &= \langle 1|H|2\rangle = \langle 1| -\frac{\hbar^2}{8\pi^2m}\nabla^2 + V_1(\vec{r}) + V_2(\vec{r})|2\rangle \\ &= \langle 1| -\frac{\hbar^2}{8\pi^2m}\nabla^2 + V_1(\vec{r})|2\rangle + \langle 1|V_2(\vec{r})|2\rangle \end{aligned}$$

Now,  $\langle 1| -\frac{\hbar^2}{8\pi^2m}\nabla^2 + V_1(\vec{r})|2\rangle = 0$  because  $\langle 1| \left( -\frac{\hbar^2}{8\pi^2m}\nabla^2 + V_1(\vec{r}) \right) = \langle 1|E_f$  and therefore

$$\langle 1| -\frac{\hbar^2}{8\pi^2m}\nabla^2 + V_1(\vec{r})|2\rangle = E_f\langle 1|2\rangle = 0.$$

Thus,  $H_{12} = \langle 1|V_2(\vec{r})|2\rangle$ . But the potential is attractive, and hence negative. Therefore,  $\beta$  is negative.

It is uncomfortable that we assumed  $\langle 1|2\rangle = 0$  but we maintain that  $\langle 1|V_2(\vec{r})|2\rangle$  isn't. But still, the orthogonality assumption can be taken away, and we can still get the same result. So the molecular state  $|\Psi_b\rangle$  has a lower energy ( $E_0 + \beta$  more negative) than  $E_0$ . It corresponds to a symmetrical combination of the basis states.

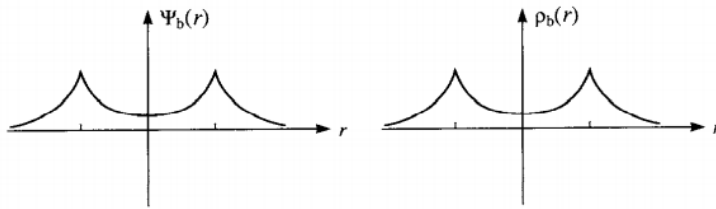


**Fig. 2.1** The wave function  $\Psi_b(r)$  and the charge density  $\rho_b(r)$  of the bonding state in a homonuclear diatomic molecule.

The two electrons in the  $H_2$  molecule occupy this molecular state, with opposite spins (the lower energy state)

Therefore, the total energy is thus lower in the molecule than for two isolated atoms by an amount of  $2|\beta|$ , this is the source of the cohesion in the molecule and that is why  $|\Psi_b\rangle$  is a bonding state.

The state  $|\Psi_a\rangle$  has energy  $E_0 - \beta$  which is greater than  $E_0$ . Since an electron occupying this state would have a higher energy than  $E_0$ , its occupation would not lead to bonding. That is why it is called the antibonding state.

### A homonuclear diatomic molecule 29

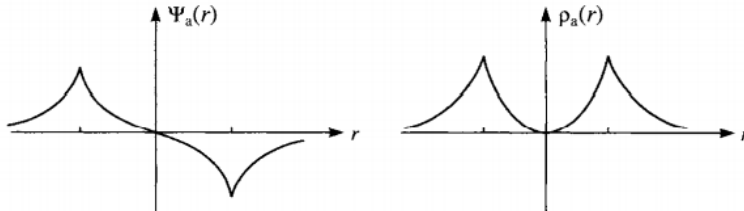


**Fig. 2.2** The wave function  $\Psi_a(r)$  and the charge density  $\rho_a(r)$  of the anti-bonding state in a homonuclear diatomic molecule.

The reason why  $|\Psi_b\rangle$  is bonding but  $|\Psi_a\rangle$  is not is clear in the figures.

The bonding state leads to more probability of electron in the region between atoms (more charge density  $\rho = |\Psi|^2$  there). Heaping up charge between the atoms leads to bonding because it is electrostatically attracted to both nuclei and therefore pulls them together.

Now we analyze the  $H_2$  molecule all over again but starting from the time-dependent Schrodinger equation. The time dependent Schrodinger equation for the state  $|\Psi\rangle$  is:

$$i\frac{\hbar}{2m}\frac{d|\Psi\rangle}{dt} = H|\Psi\rangle$$

Substituting  $|\Psi\rangle = c_1|1\rangle + c_2|2\rangle$  we obtained the following coupled first order ODE:

$$\begin{aligned} i\frac{\hbar}{2\pi}\frac{dc_1}{dt} &= H_{11}c_1 + H_{12}c_2 \\ i\frac{\hbar}{2\pi}\frac{dc_2}{dt} &= H_{21}c_1 + H_{22}c_2 \end{aligned}$$

These equations have to be solved for initial condition for  $c_1(t)$  and  $c_2(t)$ .

As before, we have that  $H_{11} = H_{22} = E_0$  and  $H_{12} = H_{21} = \beta$ . We try a solution of the type  $c_1(t) = A_1 e^{-i\omega t}$  and  $c_2(t) = A_2 e^{-i\omega t}$

When inserting them, we find two solutions for  $\omega$  corresponding to the two states:

$$\omega_b = 2\pi\frac{E_0 + \beta}{\hbar} \quad , \quad \omega_a = 2\pi\frac{E_0 - \beta}{\hbar}$$

The solutions for  $c_1(t)$  and  $c_2(t)$  are then given by

$$\left. \begin{aligned} c_1(t) &= a \exp\left(-2\pi i \frac{E_0 + \beta}{\hbar} t\right) + b \exp\left(-2\pi i \frac{E_0 - \beta}{\hbar} t\right) \\ c_2(t) &= a \exp\left(-2\pi i \frac{E_0 + \beta}{\hbar} t\right) - b \exp\left(-2\pi i \frac{E_0 - \beta}{\hbar} t\right) \end{aligned} \right\} \quad (2.40)$$

and

where  $a$  and  $b$  are arbitrary constants to be determined by the conditions at  $t = 0$ .

Suppose that at  $t = 0$  we know the molecule is in the state  $|1\rangle$  so that  $c_1(0) = 1$  and  $c_2(0) = 0$ . Then  $a = b = 1/2$  and

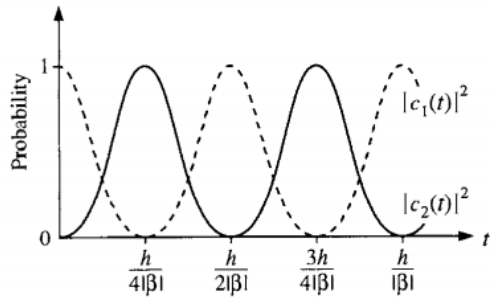
$$c_1(t) = e^{-2\pi i E_0 t / \hbar} \cos(2\pi \beta t / \hbar) \quad \text{and} \quad c_2(t) = e^{-2\pi i E_0 t / \hbar} \sin(2\pi \beta t / \hbar). \quad (2.41)$$

The two amplitudes oscillate harmonically with time. The probability that the molecule is in the state  $|2\rangle$  is given by  $|c_2(t)|^2$

$$|c_2(t)|^2 = \sin^2 \frac{2\pi \beta t}{\hbar}. \quad (2.42)$$

The probability starts at zero, as it should, and rises to one in time  $h/4|\beta|$ , and returns to zero in time  $h/2|\beta|$ , as shown in Fig. 2.3. At the same time the probability that the molecule is in the state  $|1\rangle$  is exactly out of phase, as also seen in Fig. 2.3. The number of times the molecule passes from state  $|1\rangle$  to state  $|2\rangle$  per unit time is thus  $2|\beta|/h$ . An electron in this molecular state is thus vibrating back and forth between the two atoms with period  $h/2|\beta|$ .

### A homonuclear diatomic molecule 31



**2.3** The probabilities  $|c_1(t)|^2$  (broken line) and  $|c_2(t)|^2$  (solid line) of an electron occupying the atomic states  $|1\rangle$  and  $|2\rangle$  respectively as a function of time in a diatomic molecule.

Since the ionization energy of Hydrogen is 13.6 eV, how is it possible for an electron to vibrate back and forth so freely? The answer is that the electron tunnels through the energy barrier. For this reason, the parameter  $\beta$  is called the **hopping parameter**.

We could have gotten this same solution using the time independent equation we solved before. We knew that the base solutions were:

$$\begin{aligned} |\Psi_b\rangle &= \frac{1}{\sqrt{2}}(|1\rangle + |2\rangle) \quad , \quad E_b = E_0 + \beta \\ |\Psi_a\rangle &= \frac{1}{\sqrt{2}}(|1\rangle - |2\rangle) \quad , \quad E_b = E_0 - \beta \end{aligned}$$

These are the eigenstates or stationary states of the hamiltonian  $H$  for the whole molecule,

---

so the dependent solution is:

$$\begin{aligned}
|\Psi\rangle &= a_1 e^{(E_0+\beta)it/\hbar} |\Psi_b\rangle + a_2 e^{(E_0-\beta)it/\hbar} |\Psi_a\rangle \\
&= a_1 \frac{1}{\sqrt{2}} e^{(E_0+\beta)it/\hbar} (|1\rangle + |2\rangle) + a_2 \frac{1}{\sqrt{2}} e^{(E_0-\beta)it/\hbar} (|1\rangle - |2\rangle) \\
&= \frac{1}{\sqrt{2}} (a_1 e^{(E_0+\beta)it/\hbar} + a_2 e^{(E_0-\beta)it/\hbar}) |1\rangle + \frac{1}{\sqrt{2}} (a_1 e^{(E_0+\beta)it/\hbar} - a_2 e^{(E_0-\beta)it/\hbar}) |2\rangle
\end{aligned}$$

But the initial state is  $|\Psi\rangle = c_1|1\rangle + c_2|2\rangle$ . And with that we can get the values of  $a_1$  and  $a_2$  to find the time dependence of  $|\Psi\rangle$  in the  $|\Psi_b\rangle, |\Psi_a\rangle$  basis. Or, given initial conditions, find  $c_1(t), c_2(t)$  to get the time dependence in the  $|1\rangle, |2\rangle$  basis.

## Heteronuclear Diatomic Molecule

Now suppose we have a molecule  $AB$ . Again, we will have  $H_{12} = H_{21} = \beta < 0$ .

The on-site Hamiltonian matrix elements on the  $A$  and  $B$  atoms are called  $E_A$  and  $E_B$  and we assume  $E_A > E_B$ .

Writing the atomic states as  $|A\rangle$  and  $|B\rangle$ , we suppose the molecular state is a linear combination of them:

$$|\Psi\rangle = c_A |A\rangle + c_B |B\rangle$$

The time independent Schrodinger equation  $\hat{H}\Psi = E\Psi$  now leads to:

$$\begin{aligned}
(E_A - E)c_A + \beta c_B &= 0 \\
\beta c_A + (E_B - E)c_B &= 0
\end{aligned}$$

Setting the determinant to zero for non trivial solutions for  $c_A, c_B$  again leads to a quadratic equation in  $E$  with two solutions:

$$\begin{aligned}
E_b &= \epsilon - (\Delta^2 + \beta^2)^{1/2} \\
E_a &= \epsilon + (\Delta^2 + \beta^2)^{1/2}
\end{aligned}$$

Where  $\epsilon = (E_A + E_B)/2$  and  $\Delta = (E_A - E_B)/2 > 0$ . Note that when  $\Delta = 0$ , we recover the homonuclear solution.

The effect of the difference of energies is to increase the splitting between bonding and antibonding states.

If we put these energies back onto the system of equations, we get:

In the homonuclear case the charge densities associated with each atom in both the bonding and antibonding states are equal. The charge density associated with atom 1 is proportional to  $|c_1|^2$  and it is easily seen from eqns (2.30) and (2.31) that  $|c_1|^2 = |c_2|^2 = 1/2$ . The fact that  $E_A > E_B$  in the heteronuclear molecule results in it being energetically favourable in the bonding state for some charge density to be transferred from the A atom to the B atom where it can enjoy the lower on-site energy. In the antibonding state the charge transfer is in the reverse direction. Inserting the eigenvalues, eqn (2.45), into the secular equations for the heteronuclear diatomic molecule, eqn (2.44) we find that

$$\left. \begin{aligned} \frac{c_A^2}{c_B^2} &= \frac{1}{1 + 2x^2 + 2x(1 + x^2)^{1/2}} && \text{for the bonding state} \\ \frac{c_A^2}{c_B^2} &= \frac{1}{1 + 2x^2 - 2x(1 + x^2)^{1/2}} && \text{for the antibonding state} \end{aligned} \right\} \quad (2.46)$$

Where  $x = \frac{\Delta}{\beta}$

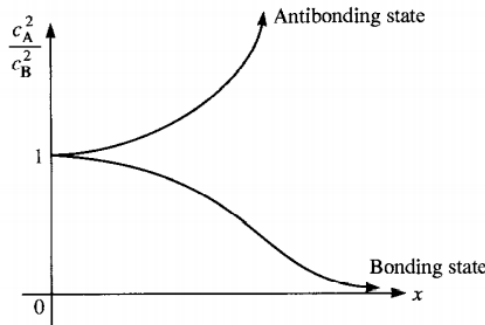


**Fig. 2.4** The ratio  $c_A^2/c_B^2$ , of the occupation of the atomic state on the A atom to that on the B atom in an AB diatomic molecule, for the bonding and antibonding molecular states as a function of  $x = \Delta/\beta = (E_A - E_B)/2\beta$ .

As  $x \rightarrow 0$ , we have that  $c_A^2/c_B^2 = 1$  for both the bonding and antibonding states as expected. For  $x \gg 1$ , we find that  $c_A^2/c_B^2 \rightarrow 0$  for the bonding state and  $c_A^2/c_B^2 \gg 1$  for the antibonding state, meaning that in the bonding state, all the charge is transferred to the B atom (as expected) and in the antibonding state, all the charge is transferred to the A atom (weird).

So, when  $\Delta$  is not zero, the bond becomes partially ionic because some charge transfer takes place.

We define the **polarity of a bond**, meaning the extent to which it is polar or ionic as:

$$\alpha_p = \frac{x}{(1 + x^2)^{1/2}}$$

And the **covalency**, meaning to which extend it is covalent as:

$$\alpha_c = \frac{1}{(1 + x^2)^{1/2}}$$

---

It follows that  $\alpha_p^2 + \alpha_c^2 = 1$

The completely ionic bond is when  $x$  tends to infinity and the completely covalent when  $x = 0$

## Electronegativity

As we saw, the difference in on-site energies of the heteronuclear diatomic molecule had as a consequence that the bonding state charge is transferred from the atom with the higher energy to the atom with the lower one.

**Electronegativity:** The power of an atom to attract electrons to itslef from neighbouring atoms.

An electronegative scale is a set of numbers, one for each element, such that if the electronegativity of atom  $A$  is greater than that of  $B$ , the electronic charge flows from  $B$  to  $A$ . Several scales are in use and we can multiply them by a scalar or shift the zero.

Pauling's scale was obtained empirically and is shown

**Table 2.1** The Pauling electronegativity values for selected elements

H						
H						
2.2						
Li	Be	B	C	N	O	F
0.98	1.57	2.04	2.55	3.04	3.41	3.98
Na	Mg	Al	Si	P	S	Cl
0.93	1.31	1.61	1.90	2.19	2.58	3.16
K	Ca		Ge	As	Se	Br
0.82	1.00		2.01	2.18	2.55	2.96
Rb					I	
0.82						2.66
Cs						
0.79						

## Bond energy and bond order

diatomic molecule. We can write the secular equations as a matrix equation in the following way

$$\begin{pmatrix} H_{AA} & H_{AB} \\ H_{BA} & H_{BB} \end{pmatrix} \begin{pmatrix} c_A \\ c_B \end{pmatrix} = E \begin{pmatrix} c_A \\ c_B \end{pmatrix} \quad (2.54)$$

where we have written the on-site energies as  $H_{AA}$  and  $H_{BB}$  and the hopping integrals as  $H_{AB}$  and  $H_{BA}$  ( $H_{AB} = H_{BA}$ ). We have already solved this equation and obtained the two eigenvalues  $E_b$  and  $E_a$  for the bonding and antibonding states. Let the eigenvectors be

$$\begin{pmatrix} c_A^b \\ c_B^b \end{pmatrix} \quad \text{and} \quad \begin{pmatrix} c_A^a \\ c_B^a \end{pmatrix}$$

for the bonding and antibonding states respectively. Thus, for the bonding state we have

$$\begin{pmatrix} H_{AA} & H_{AB} \\ H_{BA} & H_{BB} \end{pmatrix} \begin{pmatrix} c_A^b \\ c_B^b \end{pmatrix} = E_b \begin{pmatrix} c_A^b \\ c_B^b \end{pmatrix}. \quad (2.55)$$

Premultiplying both sides of this equation by the row vector  $(c_A^{b*} \quad c_B^{b*})$  we obtain

$$(c_A^{b*} \quad c_B^{b*}) \begin{pmatrix} H_{AA} & H_{AB} \\ H_{BA} & H_{BB} \end{pmatrix} \begin{pmatrix} c_A^b \\ c_B^b \end{pmatrix} = (c_A^{b*} c_A^b + c_B^{b*} c_B^b) E_b. \quad (2.56)$$

The right hand side is simply  $E_b$  because  $(c_A^{b*} c_A^b + c_B^{b*} c_B^b) = 1$  owing to the normalization condition for the bonding state. Expanding the left hand side we obtain a physically transparent breakdown of the eigenvalue

$$E_b = c_A^b c_A^{b*} H_{AA} + c_B^b c_B^{b*} H_{BB} + \{c_A^b c_B^{b*} H_{BA} + c_B^b c_A^{b*} H_{AB}\} \quad (2.57)$$

and similarly the eigenvalue of the antibonding state can be expressed as

$$E_a = c_A^a c_A^{a*} H_{AA} + c_B^a c_B^{a*} H_{BB} + \{c_A^a c_B^{a*} H_{BA} + c_B^a c_A^{a*} H_{AB}\}. \quad (2.58)$$

Using that the cs are real and  $H$  is symmetric, we have:

$$\begin{aligned} E_b &= c_A^{b2} H_{AA} + c_B^{b2} H_{BB} + [2c_A^b c_B^b H_{AB}] \\ E_a &= c_A^{a2} H_{AA} + c_B^{a2} H_{BB} + [2c_A^a c_B^a H_{AB}] \end{aligned}$$

Let us now examine what eqn (2.57) means. Since  $c_A^b c_A^{b*}$  is just the probability of finding the electron on the A atom in the bonding state, then the first term is simply the energy contribution coming from the time spent by the electron on the A atom in the bonding state. Similarly, the second term is the energy coming from the time spent on the B atom in the bonding state. The interesting term is the last term in curly brackets. This is the contribution to the eigenvalue of the bonding state from the time spent in the bond region: it is the bond energy contribution.

The bond energy contribution to the bonding eigenvalue can be expressed as  $(c_A^b c_B^{b*} + c_B^b c_A^{b*}) H_{AB} = 2c_A^b c_B^b H_{AB}$ , where we have used  $H_{AB} = H_{BA}$  and the fact that the eigenvectors are real. The term  $c_A^b c_B^b$  is simply the interference term that we discussed in eqn (2.35) and it is called the partial bond order of the AB bond. The total bond order, or just ‘bond order’, is a sum of partial bond orders taken over all occupied states. The bond energy is twice the

---

The **bond order** is the sum of all the partial bond orders  $c_A^b c_B^b$  over all occupied states. The **bond energy** is twice the bond order times the corresponding hopping integral.

bond order times the corresponding hopping integral. Thus, if there is just one electron in the molecule it half fills the bonding state and the AB bond order is  $c_A^b c_B^b$ . If there are two electrons in the molecule they can both occupy the bonding state and the bond order is  $2c_A^b c_B^b$ . If there are three electrons in the molecule then the bonding state is fully occupied and the antibonding state is half filled. The bond order is then  $2c_A^b c_B^b + c_A^a c_B^a$ . If there are four electrons (the maximum permitted by the exclusion principle) then the antibonding state is also fully occupied and the bond order is  $2(c_A^b c_B^b + c_A^a c_B^a)$  which is zero owing to the orthonormality of the eigenvectors of a hermitian matrix. The variation of the bond order with the number of electrons in an  $H_2$  molecule is shown in Fig. 2.5.

From the invariance of the trace of a matrix under a similarity transformation we know that the sum of the bonding and antibonding eigenvalues equals the trace of the original Hamiltonian, i.e.  $H_{AA} + H_{BB}$ . Adding eqns (2.57) and (2.58) we see that the sum of the terms in the curly brackets must be zero. That is, the bond energy contributions to the bonding and antibonding states cancel. Thus, if both the bonding and antibonding states are fully occupied (by two electrons each) then the total electronic energy is just  $2(H_{AA} + H_{BB})$  and there is no bond energy. This is exactly what we would expect because the bond order is zero when both the bonding and antibonding states are fully occupied.

# From the Finite to the Infinite

## Chain Molecules and k-space

We shall consider hypothetical molecules consisting of chains of many Hydrogen atoms.

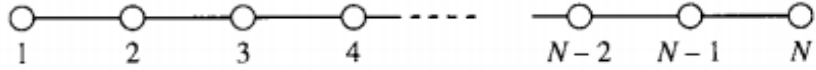


**Fig. 3.1** A linear chain of  $N$  hydrogen atoms.

Each Hydrogen atom is associated with an  $s$  state. And we assume that these states form a complete base on the  $N$  hydrogen atoms on which to expand a molecular state  $|\Psi\rangle$  as:

$$|\Psi\rangle = \sum_{j=1}^N c_j |j\rangle$$

The  $s$  state on atom  $j$  is denoted by  $|j\rangle$

We want to find the coefficients  $c_j$  and the energy of the molecular state  $|\Psi\rangle$  (the stationary states). We want to solve:

$$H|\Psi\rangle = E|\Psi\rangle$$

We insert the definition of  $|\Psi\rangle$  into the equation

$$\sum_{j=1}^N c_j H|j\rangle = E \sum_{j=1}^N c_j |j\rangle$$

And we take the  $p$ th component

$$\sum_{j=1}^N c_j \langle p|H|j\rangle = E \sum_{j=1}^N c_j \langle p|j\rangle$$

This is the **secular equation** for the chain of  $N$  atoms.

We assume that the on site states are orthogonal  $\langle p|j\rangle = \delta_{pj}$ .

For the Hamiltonian, we assume that the matrix elements are 0 except for the on-site matrix elements  $\langle p|H|p\rangle := \alpha$  and the hopping integrals  $\langle p|H|p+1\rangle = \beta$  for consecutive atoms

This gives us a set of equations:

---


$$\begin{aligned}
\alpha c_1 + \beta c_2 &= E c_1 && (\text{for } p = 1) \\
\beta c_1 + \alpha c_2 + \beta c_3 &= E c_2 && (\text{for } p = 2) \\
\beta c_2 + \alpha c_3 + \beta c_4 &= E c_3 && (\text{for } p = 3) \\
\cdots &\cdots && \\
\beta c_{j-1} + \alpha c_j + \beta c_{j+1} &= E c_j && (\text{for } p = j) \\
\cdots &\cdots && \\
\beta c_{N-2} + \alpha c_{N-1} + \beta c_N &= E c_{N-1} && (\text{for } p = N-1) \\
\beta c_{N-1} + \alpha c_N &= E c_N && (\text{for } p = N).
\end{aligned}$$

We need to solve for the coefficients  $c_j$  (the eigenvector) corresponding to possible values of  $E$  (eigenvalues).

To solve, we try a solution  $c_j = e^{ij\theta}$

It turns out that  $\theta = \frac{m\pi}{N+1}$  where  $m$  is an integer (and we therefore have  $N$  distinct solutions corresponding to  $m = 1, \dots, M$ )

The allowed energies turn out to be  $E = \alpha + 2\beta \cos\left(\frac{m\pi}{N+1}\right)$

So, we have  $N$  eigenstates (obviously), where the  $m$ th state has eigenvalue:

$$E_m = \alpha + 2\beta \cos\left(\frac{m\pi}{N+1}\right)$$

And the  $m$ th eigenvector has components:

$$c_j^{(m)} = D^{(m)} \sin\left(\frac{mj\pi}{N+1}\right)$$

Where  $D^{(m)}$  is a constant obtained by normalization  $D^{(m)} = \left(\frac{2}{N+1}\right)^{1/2}$

This general solution reproduces the eigenstates for the  $H_2$  molecule when  $N = 2$  (and the eigenvalues  $E = \alpha - \beta, \alpha + \beta$ )

$\theta$  is called the quantum number of the chain. Here we can see the spectra. When we add more and more atoms, the energy band becomes continuous.

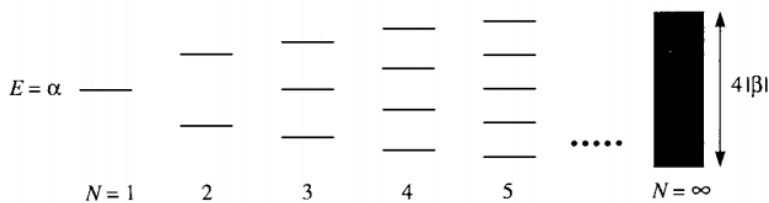


**Fig. 3.2** The eigenvalue spectra for linear chains of length  $N = 1, 2, 3, 4, 5, \dots, \infty$  hydrogen atoms. In the limit of  $N \rightarrow \infty$  a band of eigenvalues of width  $4|\beta|$  centred at  $E = \alpha$  is formed.

And here we see some wavefunctions for 5 hydrogens

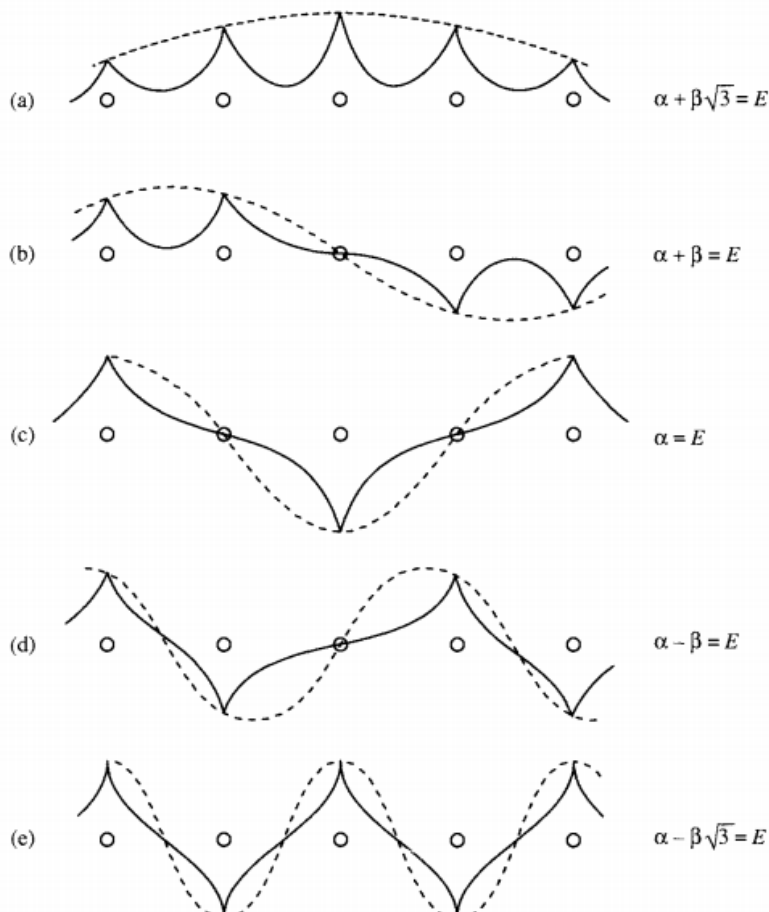


**Fig. 3.3** Molecular orbitals for the five eigenstates of the linear chain of five hydrogen atoms (shown by small circles) in order of ascending energy. The solid line shows the molecular orbital and the broken line shows the envelope  $\sin(mj\pi/6)$ , where  $m = 1, 2, \dots, 5$  in (a), (b), ..., (e), and  $j$  (which refers to the atom number) varies from 1 to 5 in each figure. Notice that as the energy increases the number of nodes in the molecular orbital increases, until, in the highest energy state (e), there is a node between every successive pair of atoms. All the molecular orbitals have nodes at atoms zero and six (not shown).

It is seen that the lowest energy state is the most bonding states with no nodes between atoms.

The next eigenstate has one node in the middle and its energy is  $\alpha + \beta$ . The next eigenstate has two nodes, at atoms 2 and 4 and energy  $\alpha$ . The 5th state, has the greatest energy and nodes in each atom.

### Infinite Chain

The same qualitative picture stands but now we discuss periodic boundary conditions. We close the chain on itself as to form a ring. The Hamiltonian is the same as before, except that atoms 1 and  $N$  are now neighbors and thus we put a Hopping  $\beta$  between them instead of 0.

With this, we model the infinite linear chain.

Now we have a similar problem but with the conditions:

$$c_0 = c_N , \quad c_{N+1} = c_1$$

Again, we propose as a solution that  $c_j = e^{ij\theta}$ . But now the boundary condition leads to  $e^{iN\theta} = 1 \Rightarrow \theta = \frac{2m\pi}{N}$  where  $m = 0, 1, 2, \dots, N - 1$

The corresponding normalized eigenstates are:

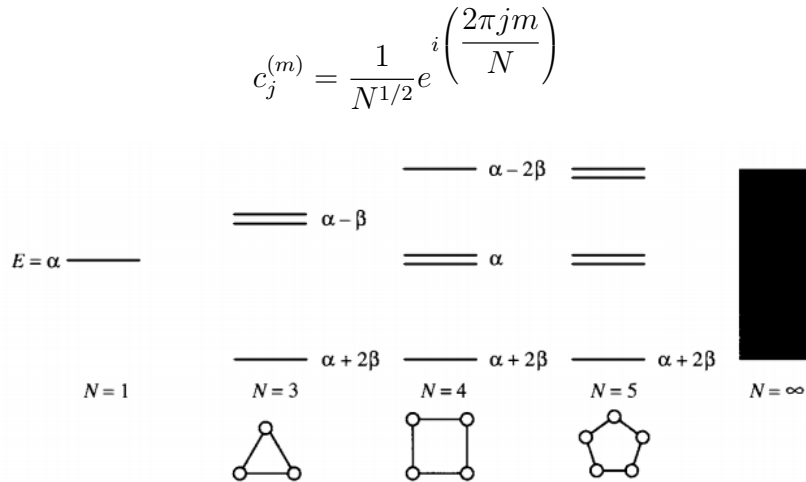


**Fig. 3.5** The eigenvalue spectra of rings of  $3, 4, 5, \dots, \infty$  hydrogen atoms. As in Fig. 3.2 the spectrum becomes a band of width  $4|\beta|$ , centred at  $E = \alpha$ , in the limit  $N \rightarrow \infty$ .

And the eigenvalues are

$$E = \alpha + 2\beta \cos\left(\frac{2\pi m}{N}\right)$$

In the infinite limit, the energies become:

$$E = \alpha + 2\beta \cos \theta$$

With a continuous variable  $\theta$  in the range  $-\pi$  and  $\pi$

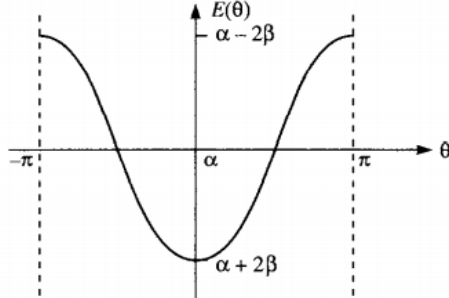


**Fig. 3.6** The eigenvalue spectrum (or band structure) for the infinite ring, plotted as a function of  $\theta$ , when there are only nearest neighbour hopping integrals.

And the expansion coefficients become:

$$c_j(\theta) = \frac{1}{N^{1/2}} e^{ij\theta}$$

We see that where  $\theta = 0$  all the expansion coefficients are equal, and therefore there are no nodes in this molecular state and this is the most bonding state. On the other hand, when  $\theta = \pm\pi$ , we see that  $c_j(\theta)$  alternates sign from one atom to the next, this is the most antibonding state.

We call all states with energy below  $\alpha$  bonding states and the rest antibonding.

### Recapitulation for the ring of $N$ atoms

By considering a ring rather than a chain of  $N$  atoms, we eliminated the edge atoms and all atoms are equivalent.

The molecular state  $|\Psi\rangle$  was then expanded as a linear combination of the  $N$  atomic states  $|j\rangle$  around the chain. The Schrodinger equation becomes a set of  $N$  coupled linear equations. We guess a solution  $c_j = e^{ij\theta}$  for the coefficients and it turns out:

- Including the normalization constant, the molecular state becomes:

$$|\Psi\rangle = \frac{1}{N^{1/2}} \sum_{j=1}^N e^{ij\theta} |j\rangle$$

- Putting into the Schrodinger equation,  $H|\Psi\rangle = E|\Psi\rangle$ , we get:

$$\sum_{j=1}^N e^{ij\theta} H |j\rangle = E \sum_{j=1}^N e^{ij\theta} |j\rangle$$

And taking the  $p$ th component:

$$\sum_{j=1}^N e^{ij\theta} \langle p | H | j \rangle = E \sum_{j=1}^N e^{ij\theta} \langle p | j \rangle$$

- 
- Using orthogonality, we get:

$$\begin{aligned} \sum_{j=1}^N e^{ij\theta} \langle p|H|j\rangle &= E e^{ip\theta} \\ \Rightarrow \sum_{j=1}^N e^{i(j-p)\theta} \langle p|H|j\rangle &= E(\theta) \end{aligned}$$

- The matrix elements  $\langle p|H|j\rangle$  are all zero except that  $\langle p|H|p\rangle = \alpha$  and  $\langle p|H|p\pm 1\rangle = \beta$ . Thus, we get that:

$$\begin{aligned} \alpha + \beta e^{i\theta} + \beta e^{-i\theta} &= E \\ \Rightarrow \alpha + 2\beta \cos \theta &= E \end{aligned}$$

- We get this answer for all values of  $p$  between 1 and  $N$ . All atoms in the ring are equivalent.

- The periodicity restriction  $c_{N+1} = c_1, c_N = c_0$  leads to  $\theta = \frac{2m\pi}{N}$

But how did we make this guess?

This is related to the **Bloch theorem**

Because of the symmetry, we should have that:

$$|\Psi(x)|^2 = |\Psi(x+m)|^2$$

Where the distance between successive atoms has been set to 1. Therefore, there must only be a phase difference:

$$\Psi(x+m) = e^{i\phi_m} \Psi(x)$$

With  $\psi_m$  the phase factor.

Now we express the wave function  $\langle x|\Psi\rangle$  in terms of the atomic orbitals  $\langle x|j\rangle$  as follows:

$$\Psi(x) = \sum_{j=1}^N c_j \langle x|j\rangle$$

And similarly for  $\Psi(x+m)$ :

$$\Psi(x+m) = \sum_{j=1}^N c_j \langle x+m|j\rangle$$

---

But  $\langle x+m|j\rangle = \langle x|j-m\rangle$ , so we have:

$$\Psi(x+m) = \sum_{j=1}^N c_{j+m} \langle x|j\rangle$$

Therefore, to satisfy the difference in phase condition, we must have:

$$c_{j+m}/c_j = e^{i\phi_m}$$

For any  $j, m$ . And since the right side depends only on  $m$ , we must have:

$$c_j = A e^{ij\theta}$$

Where  $A$  is an arbitrary constant and  $\theta$  any real number.

**Bloch's theorem** can now be stated

In the one dimensional case, if  $\Psi(x+m) = e^{im\theta}\Psi(x)$

It follows that  $\Psi(x)$  can always be represented as a periodic function, say  $p(x)$  with the periodicity of the one-dimensional lattice times  $e^{i\theta x}$ :

$$\Psi(x) = e^{i\theta x} p(x)$$

---

# Statistical Beiser

## Statistical Distribution

Statistical mechanics determines the most probable way in which a certain total amount of energy  $E$  is distributed among the  $N$  members of a system of particles in thermal equilibrium at temperature  $T$ .

We can establish how many particles have an energy  $\epsilon_1$ ,  $\epsilon_2$  and so on.

More than one particle state may correspond to a certain energy  $\epsilon$ . If the particles are not subject to the exclusion principle, more than one particle may be in a certain state.

Assumption: Each state of a certain energy is equally likely to be occupied.

A basic premise is that the greater the number  $W$  of different ways in which the particles can be arranged among the available states to yield a particular distribution of energies, the more probable is the distribution.

The program of SM begins by finding a general formula for  $W$  (the number of different ways in which we can arrange a certain distribution). The most probable distribution is the one for which  $W$  is maximum (most microstates for this macrostate), subject to the condition that the system has a fixed number  $N$  of particles whose total energy is a fixed number  $E$ . The result is then an expression for  $n(\epsilon)$ , the number of particles with the energy  $\epsilon$ .

In general:

$$\text{Number of particles of energy } \epsilon \quad n(\epsilon) = g(\epsilon)f(\epsilon)$$

Where:

- $g(\epsilon)$ = number of states of energy  $\epsilon$  (degeneracy)
- $f(\epsilon)$ : Distribution function. Average number of particles in each state of energy  $\epsilon$ . Probability of occupancy of each state of energy  $\epsilon$

If the distribution is continuous rather than discrete,  $g(\epsilon)$  is replaced by  $g(\epsilon)d\epsilon$ , the number of states the energies between  $\epsilon$  and  $\epsilon + d\epsilon$ .

- **Identical particles:** The wave functions don't overlap. They follow a **Maxwell Boltzmann distribution**
- **Identical Particles of integral spin.** Such particles, called bosons don't obey the exclusion principle, they follow the **Bose-Einstein** distribution.
- **Identical particles of half integral spin** called fermions, they follow the **Fermi Dirac** distribution

---

## Maxwell Boltzmann

It states that the average number of particles  $f_{MB}(\epsilon)$  in a state (in each state) of energy  $\epsilon$  in a system of particles at temperature  $T$  is:

$$f_{MB}(\epsilon) = Ae^{-\epsilon/kT}$$

The value  $A$  depends on the number of particles and is a normalization constante. The number  $n(\epsilon)$  of identical distinguishable particles in an assembly at temperature  $T$  that have the energy  $\epsilon$  is:

$$n(\epsilon) = Ag(\epsilon)e^{-\epsilon/kT}$$

---

### Example 9.1

A cubic meter of atomic hydrogen at 0°C and at atmospheric pressure contains about  $2.7 \times 10^{25}$  atoms. Find the number of these atoms in their first excited states ( $n = 2$ ) at 0°C and at 10,000°C.

#### Solution

(a) The constant  $A$  in Eq. (9.3) is the same for atoms in both states, so the ratio between the numbers of atoms in the  $n = 1$  and  $n = 2$  states is

$$\frac{n(\epsilon_2)}{n(\epsilon_1)} = \frac{g(\epsilon_2)}{g(\epsilon_1)} e^{-(\epsilon_2 - \epsilon_1)/kT}$$

From Eq. (7.14) we know that the number of possible states that correspond to the quantum number  $n$  is  $2n^2$ . Thus the number of states of energy  $\epsilon_1$  is  $g(\epsilon_1) = 2$ ; a 1s electron has  $l = 0$  and  $m_l = 0$  but  $m_s$  can be  $-\frac{1}{2}$  or  $+\frac{1}{2}$ . The number of states of energy  $\epsilon_2$  is  $g(\epsilon_2) = 8$ ; a 2s ( $l = 0$ ) electron can have  $m_s = \pm\frac{1}{2}$  and a 2p ( $l = 1$ ) electron can have  $m_l = 0, \pm 1$ , in each case with  $m_s = \pm\frac{1}{2}$ . Since the ground-state energy is  $\epsilon_1 = -13.6$  eV,  $\epsilon_2 = \epsilon_1/n^2 = -3.4$  eV and  $\epsilon_1 - \epsilon_2 = 10.2$  eV. Here  $T = 0^\circ\text{C} = 273$  K, so

$$\frac{\epsilon_2 - \epsilon_1}{kT} = \frac{10.2 \text{ eV}}{(8.617 \times 10^{-5} \text{ eV/K})(273 \text{ K})} = 434$$

The result is

$$\frac{n(\epsilon_2)}{n(\epsilon_1)} = \left(\frac{8}{2}\right) e^{-434} = 1.3 \times 10^{-188}$$

Thus about 1 atom in every  $10^{188}$  is in its first excited state at 0°C. With only  $2.7 \times 10^{25}$  atoms in our sample, we can be confident that all are in their ground states. (If all the known matter in the universe were in the form of hydrogen atoms, there would be about  $10^{78}$  of them, and if they were at 0°C the same conclusion would still hold.)

(b) When  $T = 10,000^\circ\text{C} = 10,273$  K,

$$\frac{\epsilon_2 - \epsilon_1}{kT} = 11.5$$

and

$$\frac{n(\epsilon_2)}{n(\epsilon_1)} = \left(\frac{8}{2}\right) e^{-11.5} = 4.0 \times 10^{-5}$$

Now the number of excited atoms is about  $10^{21}$ , a substantial number even though only a small fraction of the total.

---

---

## Molecular energies in an ideal gas

It is reasonable to consider a continuous distribution of molecular energies instead of discrete states. So  $n(\epsilon)d\epsilon$  will be the number of molecules whose energies lie between  $\epsilon$  and  $\epsilon + d\epsilon$ . Therefore:

$$n(\epsilon)d\epsilon = [g(\epsilon)d\epsilon]f(\epsilon) = Ag(\epsilon)e^{-\epsilon/kT}d\epsilon$$

The first task is to find  $g(\epsilon)d\epsilon$ , the number of available states with energy between  $\epsilon$  and  $\epsilon + d\epsilon$ . A molecule of energy  $\epsilon$  has a momentum  $p$  of  $p = \sqrt{2m\epsilon} = \sqrt{p_x^2 + p_y^2 + p_z^2}$

We imagine a momentum space with axes  $p_x, p_y, p_z$ . Then, the number of states  $g(p)dp$  with momenta with magnitudes between  $p$  and  $P + dp$  is proportional to  $4\pi p^2 dp$ . Therefore:

$$g(p)dp = Bp^2dp$$

Since each momentum magnitude  $p$  corresponds to a single energy  $\epsilon$ , the number of states  $g(\epsilon)d\epsilon$  between  $\epsilon$  and  $\epsilon + d\epsilon$  is the same as the number of momentum states between  $p$  and  $p + dp$ :

$$\begin{aligned} g(\epsilon)d\epsilon &= Bp^2dp \\ &= B(2m\epsilon)d(\sqrt{2m\epsilon}) \\ &= 2m^{3/2}B\sqrt{\epsilon}d\epsilon \end{aligned}$$

The number of molecules with energies between  $\epsilon$  and  $d\epsilon$  is then:

$$n(\epsilon)d\epsilon = C\sqrt{\epsilon}e^{-\epsilon/kT}d\epsilon$$

With  $C = AB(2m^{3/2})$

To find  $C$  we can normalize. If the total number of particles is  $N$ , then

$$N = \int_0^\infty n(\epsilon)d\epsilon = C \int_0^\infty \sqrt{\epsilon}e^{-\epsilon/kT}d\epsilon$$

We find that  $C = \frac{2\pi N}{(\pi kT)^{3/2}}$ . So finally:

$$n(\epsilon)d\epsilon = \frac{2\pi N}{(\pi kT)^{3/2}}\sqrt{\epsilon}e^{-\epsilon/kT}d\epsilon$$

Average number of molecules with energies between  $\epsilon$  and  $\epsilon + d\epsilon$  in a sample of ideal gas that contains  $N$  molecules and with temperature  $T$ .

## Average Molecular Energy

We find the average energy per molecule. For that, we calculate the total energy:

$$E = \int_0^\infty \epsilon n(\epsilon)d\epsilon = \dots = \frac{3}{2}NkT$$

So the average is:

$$\bar{\epsilon} = \frac{3}{2}kT$$

Average energy of each ideal gas molecule. The value at room temperature is about  $0.04\text{eV}$

### Equipartition of energy:

The average energy per degree of freedom of any classical object that is a member of a system in thermal equilibrium at temperature  $T$  is  $\frac{1}{2}kT$

### Distribution of molecular speeds

We have the distributions of energies, but for speeds we use  $\epsilon = \frac{1}{2}mv^2$  and  $d\epsilon = mvdv$ .

The result is that the number of particles with speeds between  $v$  and  $v + dv$  is:

$$n(v)dv = 4\pi N \left( \frac{m}{2\pi kT} \right)^{3/2} v^2 e^{-mv^2/2kT} dv$$

The speed of a molecule with the average energy of  $\frac{3}{2}kT$  is the **RMS speed**:

$$v_{rms} = \sqrt{\bar{v}^2} = \sqrt{\frac{3kT}{m}}$$

### Example 9.3

Verify that the rms speed of an ideal-gas molecule is about 9 percent greater than its average speed.

#### Solution

Equation (9.14) gives the number of molecules with speeds between  $v$  and  $v + dv$  in a sample of  $N$  molecules. To find their average speed  $\bar{v}$ , we multiply  $n(v) dv$  by  $v$ , integrate over all values of  $v$  from 0 to  $\infty$ , and then divide by  $N$ . (See the discussion of expectation values in Sec. 5.5.) This procedure gives

$$\bar{v} = \frac{1}{N} \int_0^\infty v n(v) dv = 4\pi \left( \frac{m}{2\pi kT} \right)^{3/2} \int_0^\infty v^3 e^{-mv^2/2kT} dv$$

If we let  $a = m/2kT$ , we see that the integral is the standard one

$$\int_0^\infty x^3 e^{-ax^2} dx = \frac{1}{2a^2}$$

and so

$$\bar{v} = \left[ 4\pi \left( \frac{m}{2\pi kT} \right)^{3/2} \right] \left[ \frac{1}{2} \left( \frac{2kT}{m} \right)^2 \right] = \sqrt{\frac{8kT}{\pi m}}$$

Comparing  $\bar{v}$  with  $v_{rms}$  from Eq. (9.15) shows that

$$v_{rms} = \sqrt{\frac{3kT}{m}} = \sqrt{\frac{3\pi}{8}} \bar{v} \approx 1.09\bar{v}$$

## Quantum Statistics

MB distribution holds for systems of identical particles that can be distinguished. But not all particles are like this.

- 
- **Bosons:** They have integer spin. Their wave functions should be symmetrical under exchange of a pair of elements, they are **symmetric**
  - **Fermions:** They have half integer spin. The wave function changes sign under exchange of a pair of electrons, so it is **antisymmetric**.

Consider a system of two particles 1, 2. One in state  $a$  and one in state  $b$ . If the particles are distinguishable, then the total wave function would be:

$$\begin{aligned}\psi_I &= \psi_a(1)\psi_b(2) \\ \psi_{II} &= \psi_a(2)\psi_b(1)\end{aligned}$$

If they are not distinguishable, we cannot know which one is in which state, so:

- $\psi_B = \frac{1}{\sqrt{2}}[\psi_a(1)\psi_b(2) + \psi_a(2)\psi_b(1)]$
- $\psi_F = \frac{1}{\sqrt{2}}[\psi_a(1)\psi_b(2) - \psi_a(2)\psi_b(1)]$

Suppose we want the likelihood that both particles can be in the same state, say  $a$ . For distinguishable particles both  $\psi_I$  and  $\psi_{II}$  become:

$$\psi_M = \psi_a(1)\psi_a(2)$$

To give a probability density of:

$$\psi_M^*\psi_M = \psi_a^*(1)\psi_a^*(2)\psi_a(1)\psi_a(2)$$

For bosons, the wave functions is:

$$\psi_B = \frac{1}{\sqrt{2}}[\psi_a(1)\psi_a(2) + \psi_a(1)\psi_a(2)] = \sqrt{2}\psi_a(1)\psi_a(2)$$

To give a probability density of

$$\psi_B^*\psi_B = 2\psi_M^*\psi_M$$

For fermions:

$$\psi_F = \frac{1}{\sqrt{2}}[\psi_a(1)\psi_a(2) - \psi_a(1)\psi_a(2)] = 0$$

So, in a system of bosons, they tend to band together and it is more probable that they have the same state.

In a system of fermions, they cannot have the same state, and they tend to repel.

---

## Bose Einstein and Fermi Dirac Distributions

The probability  $f(\epsilon)$  that a particles occupies a state of energy  $\epsilon$  is

- **Bose Einstein**  $f_{BE}(\epsilon) = \frac{1}{e^\alpha e^{\epsilon/kT} - 1}$

- **Fermi Dirac**  $f_{FD}(\epsilon) = \frac{1}{e^\alpha e^{\epsilon/kT} + 1}$

$\alpha$  depends on the properties of the system and may be a function of  $T$ .

It is obtained by normalizing the sum over all energy states of  $n(\epsilon) = g(\epsilon)f(\epsilon)$ .

If the number of particles is not fixed, like in photons, it turns out that  $\alpha = 0$

In both cases, when  $\epsilon \gg kT$ , the functions approach the MB statistics.

**Fermi Energy:** It is the energy where  $f_{FD}(\epsilon) = \frac{1}{2}$  (that is, it has 50% probability of being occupied). It is equal to:

$$\epsilon_F = -\alpha kT$$

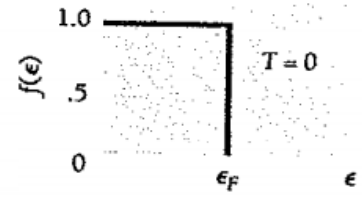
Then, the Fermi Dirac distribution becomes:

$$f_{FD}(\epsilon) = \frac{1}{e^{(\epsilon-\epsilon_F)/kT} - 1}$$

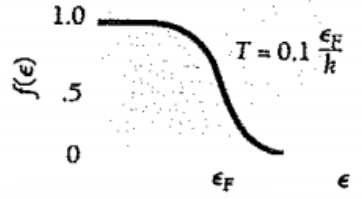
If  $T = 0$ , we find that  $f_{FD}(\epsilon) = 1$  when  $\epsilon < \epsilon_F$  and that  $f_{FD}(\epsilon) = 0$  when  $\epsilon > \epsilon_F$ .  
So the Fermi energy is the last energy occupied when  $T = 0$ .

If a system has a total of  $N$  fermions, we can calculate its Fermi energy  $\epsilon_F$  by filling up its energy state with  $N$  particles in order of increasing energy from  $\epsilon = 0$ . The highest state to be occupied will then have energy  $\epsilon = \epsilon_F$

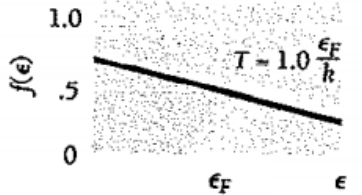
As the temperature is increased above  $T = 0$  but with  $kT$  smaller than  $\epsilon_F$ , fermions will leave states just below  $\epsilon_F$  to move into states just above it. And in higher temperatures, even particles with energies close to zero will migrate to higher energies.



(a)



(b)



(c)

**Figure 9.6** Distribution function for fermions at three different temperatures. (a) At  $T = 0$ , all the energy states up to the Fermi energy  $\epsilon_F$  are occupied. (b) At a low temperature, some fermions will leave states just below  $\epsilon_F$  and move into states just above  $\epsilon_F$ . (c) At a higher temperature, fermions from any state below  $\epsilon_F$  may move into states above  $\epsilon_F$ .

The actual number of particles  $n(\epsilon)$  with energy  $\epsilon$  is as always  $n(\epsilon) = g(\epsilon)f(\epsilon)$

**Table 9.1** The Three Statistical Distribution Functions

	Maxwell-Boltzmann	Bose-Einstein	Fermi-Dirac
Applies to systems of	Identical, distinguishable particles	Identical, indistinguishable particles that do not obey exclusion principle	Identical, indistinguishable particles that obey exclusion principle
Category of particles	Classical	Bosons	Fermions
Properties of particles	Any spin; particles far enough apart so wave functions do not overlap	Spin 0, 1, 2, . . . ; wave functions are symmetric to interchange of particle labels	Spin $\frac{1}{2}, \frac{1}{2}, \frac{1}{2}, \dots$ ; wave functions are antisymmetric to interchange of particle labels
Examples	Molecules of a gas	Photons in a cavity; phonons in a solid; liquid helium at low temperatures	Free electrons in a metal; electrons in a star whose atoms have collapsed (white dwarf stars)
Distribution function (number of particles in each state of energy $\epsilon$ at the temperature $T$ )	$f_{MB}(\epsilon) = Ae^{-\epsilon/kT}$	$f_{BE}(\epsilon) = \frac{1}{e^{\epsilon/kT} - 1}$	$f_{FD}(\epsilon) = \frac{1}{e^{(\epsilon-\epsilon_r)/kT} + 1}$
Properties of distribution	No limit to number of particles per state	No limit to number of particles per state; more particles per state than $f_{MB}$ at low energies; approaches $f_{MB}$ at high energies	Never more than 1 particle per state; fewer particles per state than $f_{MB}$ at low energies; approaches $f_{MB}$ at high energies

## Specific Heats

Let us consider the molar specific heat of a solid at constant volume,  $c_V$ . This is the energy that must be added to 1kmol of the solid, whose volume is held fixed, to raise its temperature by 1K.

The internal energy of a solid resides in the vibrations of its constituent particles, which may be atoms, ions or molecules. These vibrations may be resolved into components along three perpendicular axes, so that we may represent each atom by 3 harmonic oscillators. As we know, according to classical physics a harmonic oscillator in a system of them in thermal equilibrium at the temperature  $T$  has an average energy of  $kT$ , so each atom has  $3KT$  of energy. And the total  $n$  atoms in a mole have

**Classical internal energy of solid:**

$$E = 3nkT = 3RT$$

The specific heat at constant volume is then:

$$c_V = \left. \frac{\partial E}{\partial T} \right)_V = 3R$$

This is the **Dulong Petit law**.

This law fails for light elements such as Boron and Beryllium and carbon. worse still, the

---

specific heats of all solids drop sharply when  $T \rightarrow 0$ , so something's wrong.

### Einstein's Formula

Einstein realize the mistake of using  $kT$  as the average energy per oscillator. According to him, the probability  $f(\nu)$  that an oscillator have the frequency  $\nu$  is  $f(\nu) = \frac{1}{e^{h\nu/kT} - 1}$ . Hence the average energy for an oscillator whose frequency of vibration is  $\nu$  is:

$$\bar{\epsilon} = h\nu f(\nu) = \frac{h\nu}{e^{h\nu/kT} - 1}$$

And not  $\bar{\epsilon} = kT$ . So the total energy of a kilomole of solid is:

$$E = 3n\bar{\epsilon} = \frac{3nh\nu}{e^{h\nu/kT} - 1}$$

So we find that:

$$c_V = \frac{\partial E}{\partial T} = 3R \left( \frac{h\nu}{kT} \right)^2 \frac{e^{h\nu/kT}}{(e^{h\nu/kT} - 1)^2}$$

### Free Electrons in a Metal

In a typical metal, each atom contributes one electron to the common electron gas. So in a mole of metal, there are  $n$  free electrons. If they behave like the molecules of an ideal gas, each would have  $\frac{3}{2}kT$  of kinetic energy on the average. The metal would then have:

$$E_e = \frac{3}{2}nkT = \frac{3}{2}RT$$

of internal energy per mole due to electrons. The molar specific heat due to the electrons would then be  $c_{Ve} = \left( \frac{\partial E_e}{\partial T} \right)_V = \frac{3}{2}R$ .

According to the equation for FD, the average occupancy of a state of energy  $\epsilon$  in a system of fermions is:

$$f_{FD}(\epsilon) = \frac{1}{e^{(\epsilon-\epsilon_F)/kT} - 1}$$

What we also need is  $g(\epsilon)d\epsilon$ , the number of available states to electrons with energies between  $\epsilon$  and  $\epsilon + d\epsilon$ .

The number of standing waves in a cubical cavity  $L$  on a side is:

$$g(j) dj = \pi j^2 dj$$

Where  $j = 2L/\lambda$ , where in the case of an electron,  $\lambda = h/p$ . Therefore, we have:

$$j = \frac{2L\sqrt{2m\epsilon}}{h} , \quad dj = \frac{L}{h}\sqrt{\frac{2m}{\epsilon}}d\epsilon$$

Then, we have that:

$$g(\epsilon)d\epsilon = \frac{8\sqrt{2}\pi V m^{3/2}}{h^3} \sqrt{\epsilon} d\epsilon$$

## Fermi Energy

The final step is to calculate the  $\epsilon_F$ . We can do this by filling up the energy states at  $T = 0$  with the  $N$  free electrons in order of increasing energy starting from  $\epsilon = 0$ . The highest state to be filled will have an energy of  $\epsilon = \epsilon_F$ . Hence:

$$N = \int_0^{\epsilon_F} g(\epsilon)d\epsilon = \dots = \frac{16\sqrt{2}\pi V m^{3/2}}{3h^3} \epsilon_F^{3/2}$$

Then:

$$\epsilon_F = \frac{h^2}{2m} \left( \frac{3N}{8\pi V} \right)^{2/3}$$

### Example 9.8

Find the Fermi energy in copper on the assumption that each copper atom contributes one free electron to the electron gas. (This is a reasonable assumption since, from Table 7.4, a copper atom has a single 4s electron outside closed inner shells.) The density of copper is  $8.94 \times 10^3 \text{ kg/m}^3$  and its atomic mass is 63.5 u.

#### Solution

The electron density  $N/V$  in copper is equal to the number of copper atoms per unit volume. Since  $1 \text{ u} = 1.66 \times 10^{-27} \text{ kg}$ ,

$$\begin{aligned} \frac{N}{V} &= \frac{\text{atoms}}{\text{m}^3} = \frac{\text{mass}/\text{m}^3}{\text{mass}/\text{atom}} = \frac{8.94 \times 10^3 \text{ kg/m}^3}{(63.5 \text{ u}) \times (1.66 \times 10^{-27} \text{ kg/u})} \\ &= 8.48 \times 10^{28} \text{ atoms/m}^3 = 8.48 \times 10^{28} \text{ electrons/m}^3 \end{aligned}$$

The corresponding Fermi energy is, from (9.56),

$$\begin{aligned} \epsilon_F &= \frac{(6.63 \times 10^{-34} \text{ J} \cdot \text{s})^2}{(2)(9.11 \times 10^{-31} \text{ kg/electron})} \left[ \frac{(3)(8.48 \times 10^{28} \text{ electrons/m}^3)}{8\pi} \right]^{2/3} \\ &= 1.13 \times 10^{-18} \text{ J} = 7.04 \text{ eV} \end{aligned}$$

At absolute zero,  $T = 0 \text{ K}$ , there would be electrons with energies of up to 7.04 eV in copper (corresponding to speeds of up to  $1.6 \times 10^6 \text{ m/s!}$ ). By contrast, all the molecules in an ideal gas at 0 K would have zero energy. The electron gas in a metal is said to be **degenerate**.

## Electron Energy Distribution

We have that the number of electrons in an electron gas that have energies between  $\epsilon$  and  $\epsilon + d\epsilon$  is:

$$n(\epsilon)d\epsilon = g(\epsilon)f(\epsilon)d\epsilon = \frac{(8\sqrt{2}\pi V m^{3/2}/h^3)\sqrt{\epsilon}d\epsilon}{e^{(\epsilon-\epsilon_F)/kT} + 1}$$

Or using the expression for  $\epsilon_F$ , we have:

$$n(\epsilon)d\epsilon = \frac{(3N/2)\epsilon_F^{-3/2}\sqrt{\epsilon}d\epsilon}{e^{(\epsilon-\epsilon_F)/kT} + 1}$$

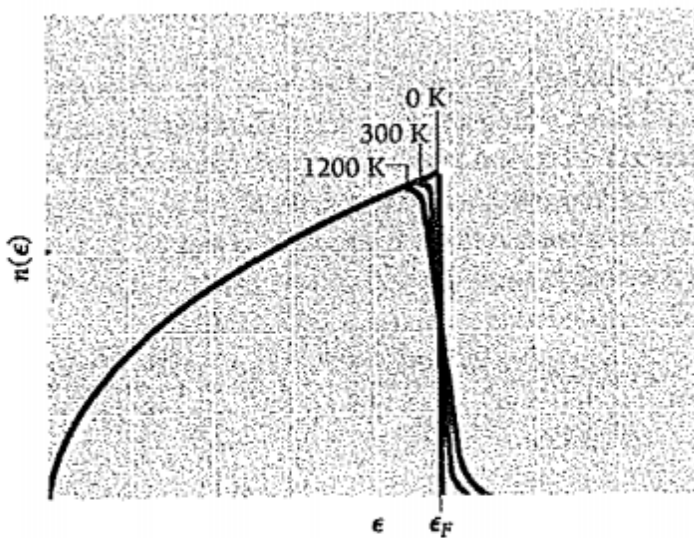


**Figure 9.11** Distribution of electron energies in a metal at various temperatures.

Let's determine the average electron energy at 0K. We first calculate the total energy  $E_0$  at 0K, it is  $E_0 = \int_0^{\epsilon_F} \epsilon n(\epsilon)d\epsilon = \dots = \frac{3}{5}N\epsilon_F$ . Therefore,  $\bar{\epsilon}_0 = \frac{3}{5}\epsilon_F$

---

# The Solid State

## Crystalline and Amorphous Solids

Solids are **crystalline** if they are composed of regular, repeated 3D patterns, they have long range order.

Solids that lack these types of arrangements are called **amorphous**. They do exhibit **short range order**

## Crystal Defects

In a perfect crystal each atom has a definite equilibrium location in a regular array. Actual crystals are never perfect. The simplest category of crystal imperfection is the point defect. A dislocation is a type of crystal in which a line of atoms is not in its proper position, they can happen by edge dislocation or screw dislocation.

## Band Theory of Solids

Conductivity varies widely between solids.

## Conductors

the figure shows the energy levels and bands in sodium. The 3s level is the first occupied level to broaden into a band.

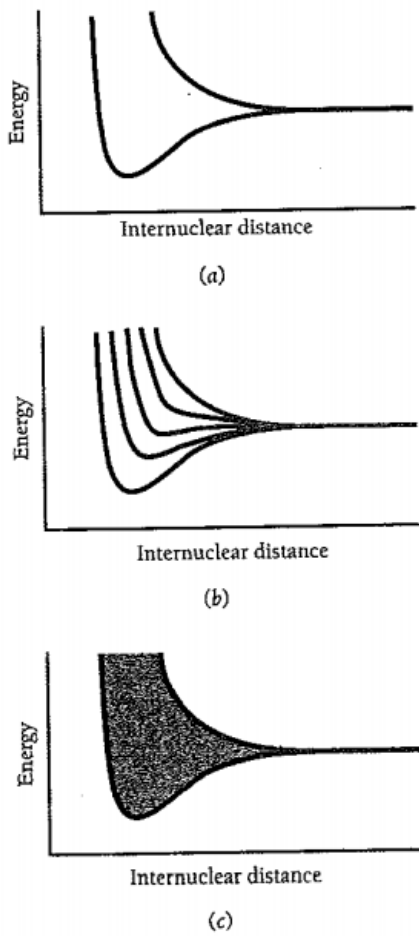


**Figure 10.19** The 3s level is the highest occupied level in a ground-state sodium atom. (a) When two sodium atoms come close together, their 3s levels, initially equal, become two separate levels because of the overlap of the corresponding electron wave functions. (b) The number of new levels equals the number of interacting atoms, here 5. (c) When the number of interacting atoms is very large, as in solid sodium, the result is an energy band of very closely spaced levels.

An electron in a solid can have energies that fall within its energy bands. The various outer energy bands in a solid may overlap, in which case its valence electrons have available a continuous distribution of permitted energies. In other solids the bands may not overlap and the intervals between them are **band gaps**.

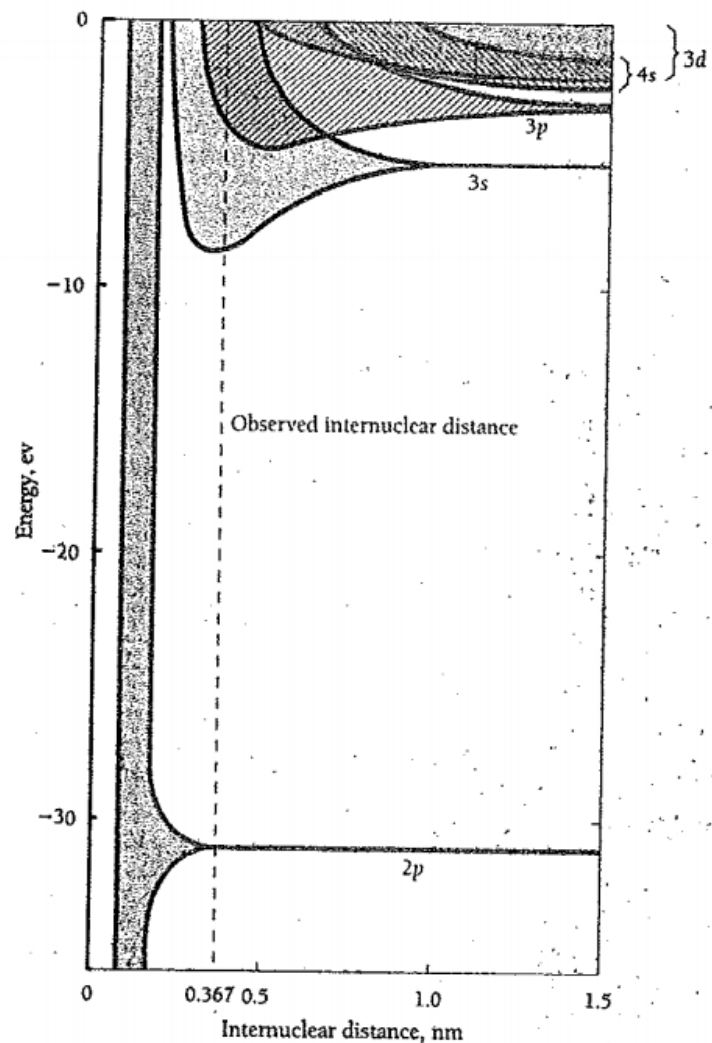
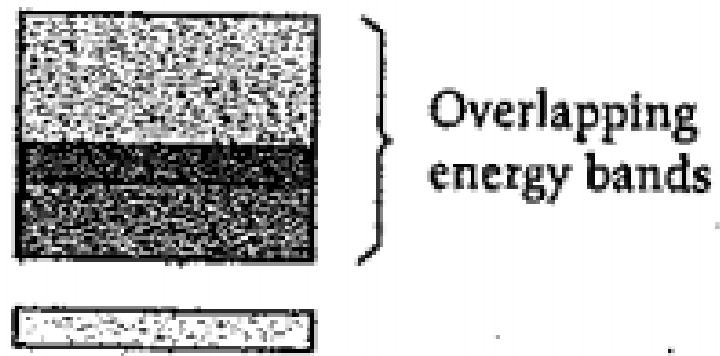
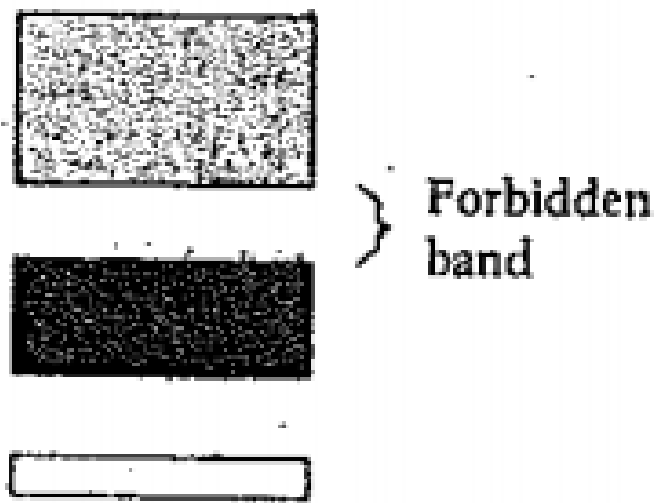


Figure 10.20 The energy levels of sodium atoms become bands as their internuclear distance decreases. The observed internuclear distance in solid sodium is 0.367 nm.



(a)



(b)

Figure 10.21 (a) The energy bands in some solids may overlap to give a continuous band. (b) A forbidden band separate nonoverlapping energy bands in other solids.

Figure 9.11 shows the distribution of electron energies in a band at various temperatures. At 0K all levels in the band are filled by electrons up to the Fermi energy  $\epsilon_F$ , and those above are empty. At temperatures above 0K, electrons with energy below  $\epsilon_F$  may move into higher states, in which case  $\epsilon_F$  represents a level with 50 % likelihood of being occupied.

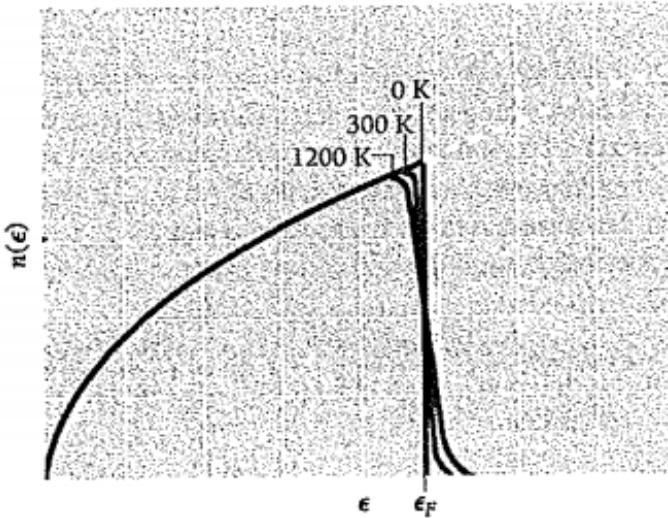


Figure 9.11 Distribution of electron energies in a metal at various temperatures.

## Insulators

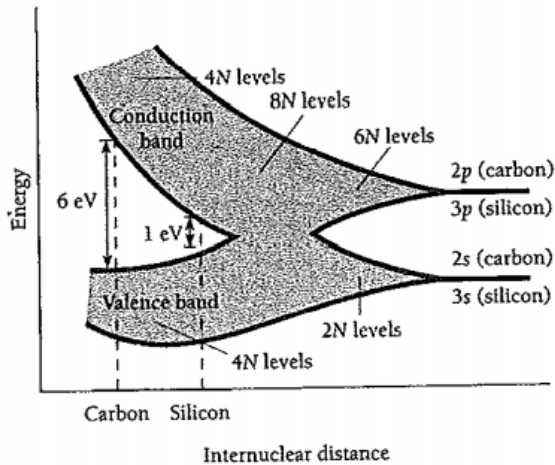
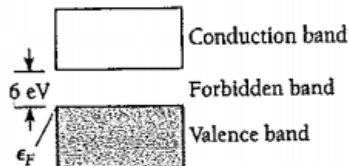


Figure 10.23 Origin of the energy bands of carbon and silicon. The 2s and 2p levels of carbon atoms and the 3s and 3p levels of silicon atoms spread into bands that first overlap with decreasing atomic separation and then split into two diverging bands. The lower band is occupied by valence electrons and the upper conduction band is empty. The energy gap between the bands depends on the internuclear separation and is greater for carbon than for silicon.

In a carbon atom the 2p shell contains only 2 electrons, because 2p can hold 6 electrons, we might think that carbon is a conductor. What actually happens is that, although the 2s and 2p bands overlap at first, at smaller separations the combined band splits into two bands,

each able to contain  $4N$  electrons.

The empty **conduction band** above the valence band is separate from it by a forbidden band 6eV wide. Here the **Fermi energy**  $\epsilon_F$  is at the top of the valence band. At least 6eV of additional energy must be provided to an electron in diamond if it is to climb to the conduction band.



**Figure 10.24** Energy bands in diamond. The Fermi energy is at the top of the filled lower band. Because an electron in the valence band needs at least 6 eV to reach the empty conduction band, diamond is an insulator.

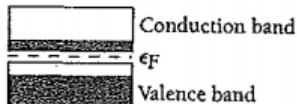


**Figure 10.25** The valence and conduction bands in a semiconductor are separated by a smaller gap than in the case of an insulator. Here a small number of electrons near the top of the valence band can acquire enough thermal energy to jump the gap and enter the conduction band. The Fermi energy is therefore in the middle of the gap.

## Semiconductors

It has a very small forbidden band, so it has a conductivity between that of conductors and that of insulators.

## Energy Bands: Alternative Analysis

This is a very different approach to the origin of energy bands than that discussed earlier about the broadening of energy levels when atoms come together.

We will bring an intuitive approach.

First, the free electron momentum is  $\lambda = \frac{h}{p}$

Unbound low energy electrons can travel freely through a crystal since their wavelengths are long relative to the lattice spacing  $a$ . More energetic electrons, such as those close to the Fermi energy have wavelengths comparable with  $a$

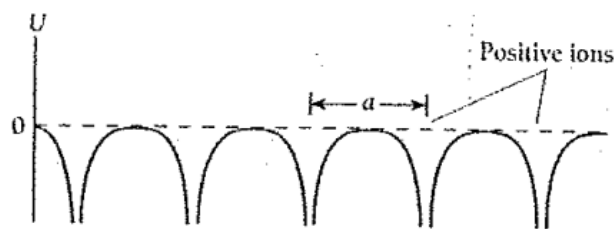


Figure 10.39 The potential energy of an electron in a periodic array of positive ions.

An electron of wavelength  $\lambda$  undergoes Bragg reflection from one of the atomic planes in a crystal when it approaches the plane at an angle  $\theta$ , where:

$$n\lambda = 2a \sin \theta \quad , \quad n = 1, 2, 3 \dots$$

We usually replace  $\lambda$  for  $k = \frac{2\pi}{\lambda}$ . So we have that:

$$k = \frac{n\pi}{a \sin \theta}$$

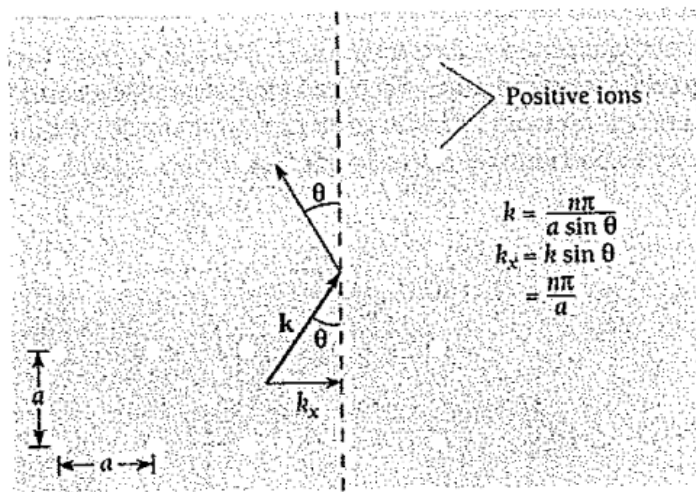


Figure 10.40 Bragg reflection from the vertical rows of ions occurs when  $k_x = n\pi/a$ .

## Brillouin Zones

The region in  $k$ -space that low- $k$  electrons can occupy without being diffracted is called the **first Brillouin zone**. The second one is also shown, it contains electrons with  $k > \pi/a$  that do not fit into the first zone yet which have sufficiently small wave numbers to avoid diffraction by the diagonal sets of atomic planes.

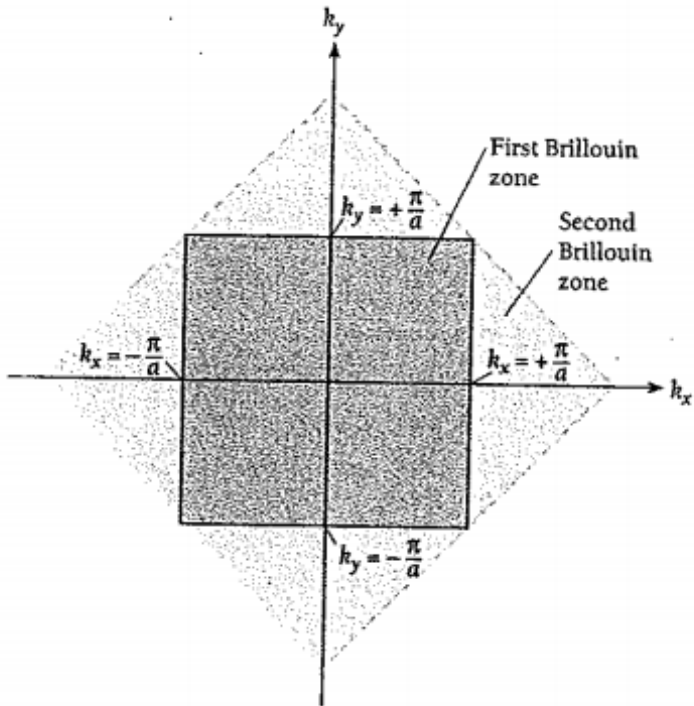


Figure 10.41 The first and second Brillouin zones of a two-dimensional square lattice.

### Origin of Forbidden Bands

# Artículo 1



RESEARCH ARTICLE

## Superconductivity in Bismuth. A New Look at an Old Problem

Zaahel Mata-Pinzón<sup>1\*</sup>, Ariel A. Valladares<sup>1,2\*</sup>, Renela M. Valladares<sup>2</sup>, Alexander Valladares<sup>2</sup>

**1** Departamento de Materia Condensada y Criogenia, Instituto de Investigaciones en Materiales, Universidad Nacional Autónoma de México, México, D.F., México, **2** Departamento de Física, Facultad de Ciencias, Universidad Nacional Autónoma de México, México, D.F., México

\* These authors contributed equally to this work.

\* [valladar@unam.mx](mailto:valladar@unam.mx)

### Abstract

A **216-atom amorphous structure (a-Bi216)** was computer generated using our **undermelt-quench approach** to investigate the relationship of the **atomic topology**, vibrational and electronic properties and superconductivity of **bismuth**.

Its **pair distribution** function compares well with experiment. The calculated **electronic density of states (eDOS)** and **vibrational density of states (VDOS)** shows that the **amorphous eDOS** is about 4 times the **crystalline** at the **Fermi Energy**. Whereas for the vDOS, the energy range of the amorphous is roughly the same as the crystalline but the shapes are different.

A simple **BCS** estimate of the possible **crystalline superconducting transition temperature** gives an upper bound of 1.3mK.

The **e-ph coupling** is more preponderant in a-Bi than in crystalline bismuth (x-Bi) as indicated by the  $\lambda$  obtained via **McMillan's formula**  $\lambda^c = 0.24$  and experiment  $\lambda^a = 2.46$ . Therefore, with respect to x-Bi, superconductivity in a-Bi is enhanced by the higher values of  $\lambda$  and of eDOS at the Fermi energy

### Introduction

Amorphous Bismuth (a-Bi) is considered a conventional superconductor, discovered several decades ago with a critical temperature of  $T_c = 6K$ , whereas the crystalline counterpart (x-Bi) has not been found yet to superconduct (above  $10^{-2}K$ ).

This put the subject in the foreground decades ago, but then it faded into the background as it was not possible to understand the dichotomy observed in the two phases. For this reason bismuth is an interesting material for studying the influence of the structure-property relations on superconductivity.

---

In the **BCS approach**, superconductivity is a collective phenomenon that invokes an e-e attractive interaction mediated by phonons and the coherent motion of these electronic **Cooper pairs**.

So, studying the electronic and vibrational properties of the two Bi phases may disentangle the mystery of their different behaviors and shed light on other amorphous superconducting systems where the crystalline counterparts have not yet been found to superconduct.

BSC has many opponents. Since superconductors with high  $T_c$  cast doubts on the mechanism to generate electron pairs, since it is argued that according to the BCS theory, the transition temperature would be, at best, of the order of the **Debye temperature** of the material.

Nevertheless, it is common to accept the BCS formalism for 'normal' low  $T_c$  superconductors, since it has predicting power in this realm.

Despite its successes, the BCS theory has not been able to foretell which materials would be superconductors and their  $T_c$  due to the difficulty in calculating the e-ph coupling potential from first principles.

In this work, we report upper bound values for the transition temperature of a given phase if this temperature is known for the other phase and if we can calculate the electronic and vibrational properties of both phases.

The manner in which amorphous samples are generated varies widely. Some methods consider liquefying the samples and then cooling them below their melting points, but this sometimes leads to samples with some remnants characteristics of the liquid state.

To avoid this, we devised the new approach **undermelt quench** process. It consists of heating 'crystalline' unstable supercells with the correct density, to temperatures just below the melting value of the real material. A **cooling ramp** is then applied to the disordered sample with a cooling rate that has the same value as that of the heating ramp. If necessary, **relaxing cycles** are applied so that at the end, the **energy optimization process** leads to an amorphous structure that is in a **metastable state**.

A structural property determined for amorphous materials is the **radial or pair distribution function (PDF,  $g(r)$ )** obtained experimentally by diffraction methods.

A drawback is that since they are averaged one dimensional quantities, it is argued that some disordered topologies lead to indistinguishable PDFs. There is a need to computer generate reliable amorphous structures with PDFs in agreement with experiment and that allow the calculation of physical properties. We have done this for the case of bismuth (computer generated a sample, calculated PDFs that agree with experiment, predicted electronic and vibrational properties of both phases to see the influence on superconductivity).

Since 1950 several authors experimentally determined PDFs of Bismuth. They agree that

---

the structure of a-Bi is very similar to the corresponding liquid. In 1969 Fujime characterized his sample and gave the following arguments to say that his bismuth was amorphous:

- The PDF has 3 peaks. One at 3.28 Å, 4.5 Å and 6.5 Å
- **Coordination number of  $N = 5.6$** , where  $N$  was obtained by integrating a Gaussian-like curve adjusted to the first peak of  $J(r) = 4\pi r^2 g(r)$ .

In computer generation, realistic QM forces have to be calculated using QM methos like the **ab initio DFT** approach.

But this is so computer intensive that the size of the structures are restricted to a few hundred atoms.

## Methods

### Structural Simulation

We perform simulated **annealing processes** using the **Fastructure code** and the **Harris Functional**, a **DFT** calculation. Also the **Local Density Approximation (LDA)**, with the parametrization of **Vosko, Wilk and Nusair (VWN)**.

The calculations are carried out with an all electron basis, within the frozen core approximation.

Since Bismuth has 83 electrons, the **valence states** are described via a minimal basis set of "finite range" atomic orbitals with a cutoff radius of 5Å, which is large enough to include fourth neighbors in the crystalline structure.

The forces are calculated using rigorous formal derivatives of the expression for the energy in the **Harris funcitonal**.

The amorphous structures are computer generated using a slight modification of the under-melt quench method. Starting from an unstable crystalline **diamond** like supercell with 216 atoms of bismuth (a-Bi<sub>216</sub>) and a volume of 7645.37Å<sup>3</sup> (19.7Å per edge).

The parameters of the starting structure are adjusted to assure that the interatomic distances are close to those in  $x - Bi$  and that the density is close to 9.8g/cm<sup>3</sup> (the density of  $x - Bi$ ), so the final supercell is in solid state.

Since  $x - Bi$  has a **rhombohedral structure**, the diamond like structure is unstable and will disorder as the temperature is raised.

At temperatures just below the melting point the structure is totally disordered, but upon cooling the tendency to crystallization appears so the **time state** has to be chosen carefully to avoid this process.

The simulated annealing processes are carried as follows:

- The initial diamond-like supercell is heated from 300K to 540K (4.5 K below Bismuth melting point) in 100 computational steps.

- 
- Then it is **quenched** from 540 K to close to 0K in 225 steps, in order to maintain the same temperature rate in heating and cooling (2.4 K per step)
  - When cooling, the disordered structure gets into a metastable topology that leads to an amorphous state.
  - A **geometry optimization** using **DMol** is performed to guarantee that the amorphous structure is at an energy minimum, representing a **metastable** amorphous solid.

When using DMol3 we use the computation time scales with a high power of the cutoff radius, because the **time-limiting** factor of the runs is the number of **three-center integrals** that have to be computed using the **weight-function method of Delley**

In all cases **periodic boundary conditions** are utilized.

For the x-Bi we take the structure given by **Wyckoff** and repeat it 6x6x3 times to obtain a 216 atom **crystalline supercell** (x-Bi216).

This was done to have the same number of atoms per supercell so that the properties of a-Bi and x-Bi can be directly compared.

We then calculate the **radial distribution function**  $g(r)$  and compare it to experiment. IF simulation and experiment agree, we then proceed to calcualte the electronic and vibrational densities of states eDOS and vDOS of both the crystalline and amorphous samples.

## Electronic and Vibrational Simulations

We first generate the atomic topology of the material using our underlment quench approach and then calculate the properties using **density functional first principles** techniques. Since we use a supercell, electron energy levels are obtained and the density of electronic states calculated by counting the number of states per unit energy. Vibrational frequencies are calculated with DMol3 for the 216-atom crystalline and amorphous supercells.

The method used was the finite displacement approach. The curves were smoothed so that the number of frequencies equals  $3N_a$  with  $N_a$  the number of atoms in the supercells.

To compare with experiment, we built the vDOS for x-BI digitizing the points on the dispersion curves collected from several experiments and processed it in the same manner as our data. We also compare our data with the experimental vDOS reported for a temperature of 77K.

To obtain the electronic and vibrational properties a **single-point energy calculation** has to be carried out first. These single-point energy calculations are performed with the DMol3 code in the Materials Studio suite using a double numeric basis set and a finer mesh within

the VWN approximation.

An unrestricted **spin-polarized calculation** for the energy was carried out, leaving out the Harris functional approach.

Since Bismuth is a heavy element, the **density functional semi core pseudo potential (DSPP)** approximation was used. Since DSPPs have been designed to generate accurate DMol3 calculations, it is expected that their use represents a good approximation.

The resulting crystalline eDOS and vDOS were compared with experimental data available, this would validate our results for the amorphous supercell. We then compare the results for the amorphous and the crystalline cells and through this comparison suggest a reason as to why the amorphous and crystalline phases have different superconducting properties. We also infer a possible upper bound for the superconducting transition temperature of x-Bi.

## Results and Discussion

### Structure

We obtain a 216-atom amorphous structure of bismuth (a-Bi216) by simulated **annealing** a 216-atom unstable crystalline supercell, using a slight modification of the undermelt quench approach.

We calculate the PDF of the resulting amorphous structure.

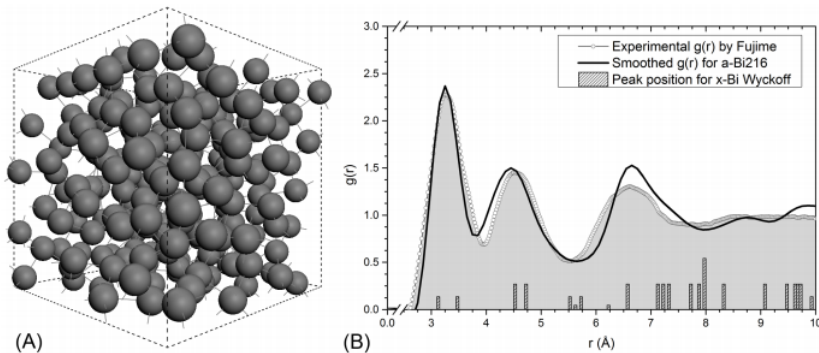


**Fig 1. Structural analysis of simulated a-Bi.** (A) Computer-generated amorphous supercell of bismuth, a-Bi216. (B) Computational  $g(r)$  for a-Bi216 compared with the experimental results obtained by Fujime [2]. Positions of the peaks for the rhombohedral x-Bi are included for contrast with the broader, amorphous ones.

We compare the PDF with the experimental result, which reveals an exceptional agreement with the experimental PDF. Positions and relative errors are as follows:

The relative error for the first peak position (3.25 Å) is 0.91 %, for the second (4.45 Å) is 1.11% and for the third (6.65 Å) 2.26%.

This indicates that the amorphous structures generated possess PDFs in agreement with experiment.

Notice that the first amorphous peak (3.25 Å) is at almost the average distance of the first two crystalline peaks (3.11 Å, 3.45 Å). This implies that the first two crystalline peaks coalesce

into a single amorphous peak. A similar situation occurs for the second amorphous peak where the third and fourth crystalline peaks coalesce.

Shoulders in the first and second of  $g(r)$  are commonly encountered in metallic glasses, but a-Bi does not have marked shoulders due perhaps to its peculiar bonding, somewhat covalent and somewhat metallic.

The **Plan Angle Distribution PAD** for the a-Bi<sub>216</sub> supercell shows that the maximum is located at 82.5 degrees. The shape of the PAD calculated here is very different from the typical PAD obtained for amorphous metals, since for these metallic materials, the distribution displays two preponderant peaks at 60 and 116 degrees.

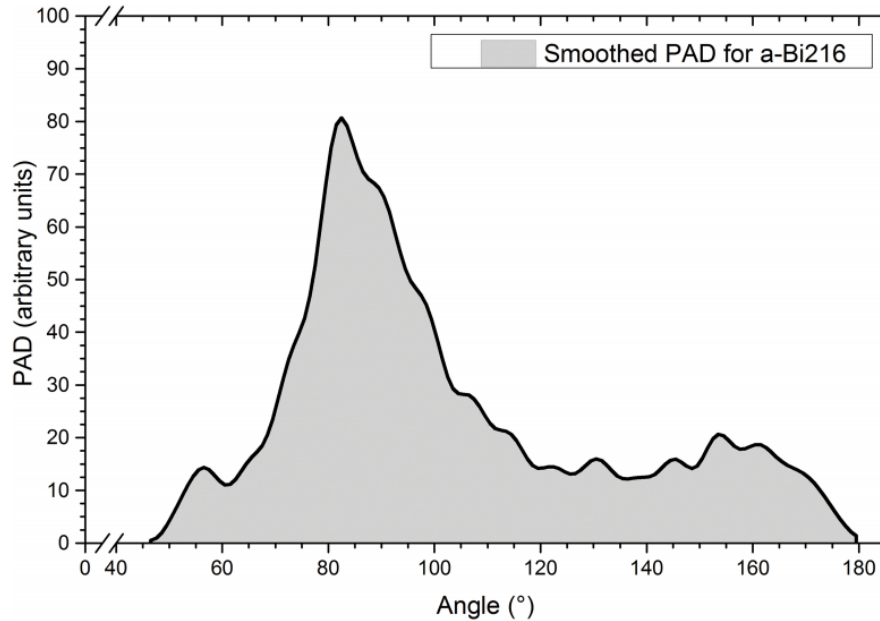


**Fig 2. PAD for the a-Bi<sub>216</sub> supercell.** The nearest neighbor values of the plane angle in x-Bi are 89° and 91°, whereas the maximum for the amorphous cell occurs at 82.5°. Notice the shoulder located at 56.5° which is reminiscent of angles in an equilateral triangular structure. The bump at about 155° may be due to non-planar surfaces bounding deformed cubes in this amorphous structure.

As was done for the  $g(r)$ , the PAD was obtained from the nuclei positions in the amorphous supercell. The criterion assumed is that the atoms are bonded when they are located at distances  $\leq 3.8\text{\AA}$ , which is the distance for the first minimum in the a-Bi<sub>216</sub> PDF. The smoothing was done using a **3 point Fast Fourier filter** using Origin 9.

Semi planar structures can be associated with peaks in the neighborhood of 155°, triangles with peaks near 56.5° and cubic like structures with peaks near 82°.

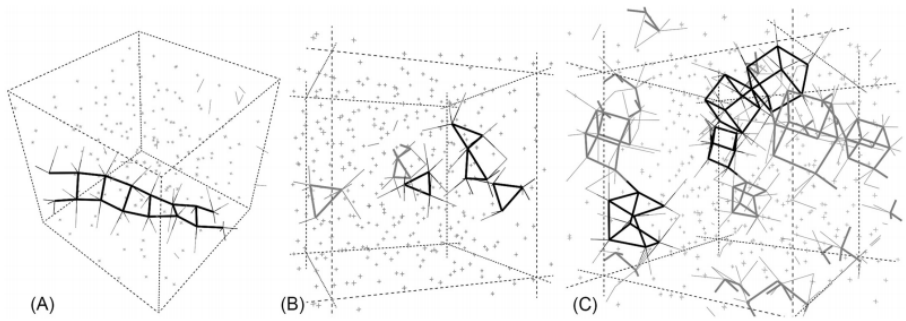


**Fig 3. Some structures within a-Bi216.** (A) Semi-planar structure associated with angles in the neighbourhood of 155°. (B) Triangular structures associated with the bump at 56.5°, reminiscent of quasi-equilateral triangles. (C) Deformed cubic-like arrangements reminiscent of the crystalline structure of bismuth, corresponding to 82°. Linked atoms are nearest neighbors.

## Electronic and Vibrational Properties

There are no other theoretical or computational results for a-Bi. So we present the results we got for the structure that led to the PDF in agreement with experiment. Our accumulated results show that the undermelt-quench method is a good approach for generation of amorphous topologies. So we trust the results for EDOS and VDoS we get here, though there is no comparison.

However, there are results for crystalline, which we will use for comparison.

We show the eDOS calculated for x-Bi216 and compare it with experimental data obtained by **Angle Resolved Photo Emission Spectroscopy (ARPES)**, **X-ray Photoelectron Spectroscopy (XPS)** and **Ultraviolet Photoelectron Spectroscopy (UPS)**

Two bands are presented, the s band (from -14 eV to -8 eV) and the p band (from -5 eV to 6 eV)

For the s-band a split appears in all the theoretical and experimental results. Also, for the p-band we get a split before the **Fermi energy** and this separation is a consequence of the spin orbit coupling of the p orbitals.

because x-Bi is a **semimetal** we get a **pseudo gap** at the **Fermi energy (Fermi level)** in the theoretical results.

Thus our calcualted eDOS for the crystalline structure reproduces the experiment and validates the experimental eDOS.

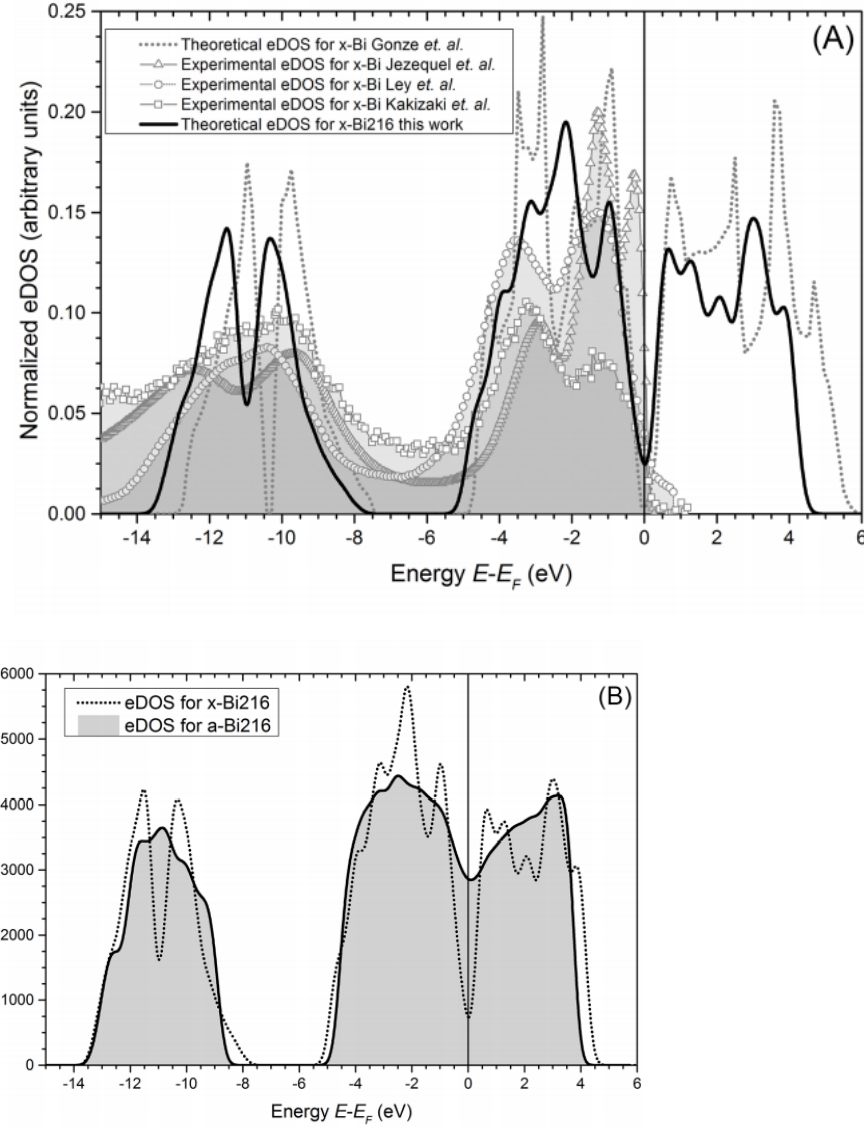


**Fig 4. Electronic crystalline and amorphous behavior.** (A) Comparison of our normalized result for  $x\text{-Bi}216$  with the theoretical eDOS for  $x\text{-Bi}$  from Gonze *et al.* [32] and the experimental data taken from Jezequel *et al.* [30], Ley *et al.* [22] and Kakizaki *et al.* [31]. Normalization indicates that the area under each curve, up to the Fermi level,  $E_F - E = 0$ , is set equal to 1. (B) The calculated eDOS for the amorphous structure  $a\text{-Bi}216$  (full line) and for the crystalline  $x\text{-Bi}216$  (dotted line) are shown; the relevant feature for the amorphous is that the pseudo-gap has essentially disappeared and that therefore there are more electrons at  $N(E_F)$  in  $a\text{-Bi}$  than in  $x\text{-Bi}$ .

For the  $x\text{-Bi}$  two bands can be identified, the s band and the p band but both smoother. The narrow peaks that appear in the crystalline results are now washed out due to a more homogeneous environment in the amorphous.

The split peaks for the s and p band have disappeared as has the pseudo gap.

In fig 4B a substantial increment in the density of electronic states at the Fermi level,  $N(E_F)$ , for the amorphous is observed (it is an increment of 388% in the density of states at the Fermi level compared to crystalline).

Still, in an amorphous material, disorder causes localization of the electrons and although there are more states at the Fermi level, they may not be mobile.

Nevertheless, it is clear that there are more electrons at  $N(E_F)$  in the amorphous than in the crystalline bismuth.

Some authors have determined the **electron phonon coupling function** of a-Bi by **McMillans inversion procedure**. But the pure vibrational density of states (vDOS or  $F(\omega)$ ) for the amorphous has never been reported.

We get a result for crystalline similar to experiment and thus validate the amorphous one. The  $F(\omega)$  for the amorphous sample presents marked differences with respect to x-Bi. We obtain a presence between 0 and 4 meV of a large number of acoustic (soft) phonon modes. Next, the gap between the acoustic and optical branches. Finally, the extension of the vDOS on the energy scale is somewhat reduced compared with crystalline curve.

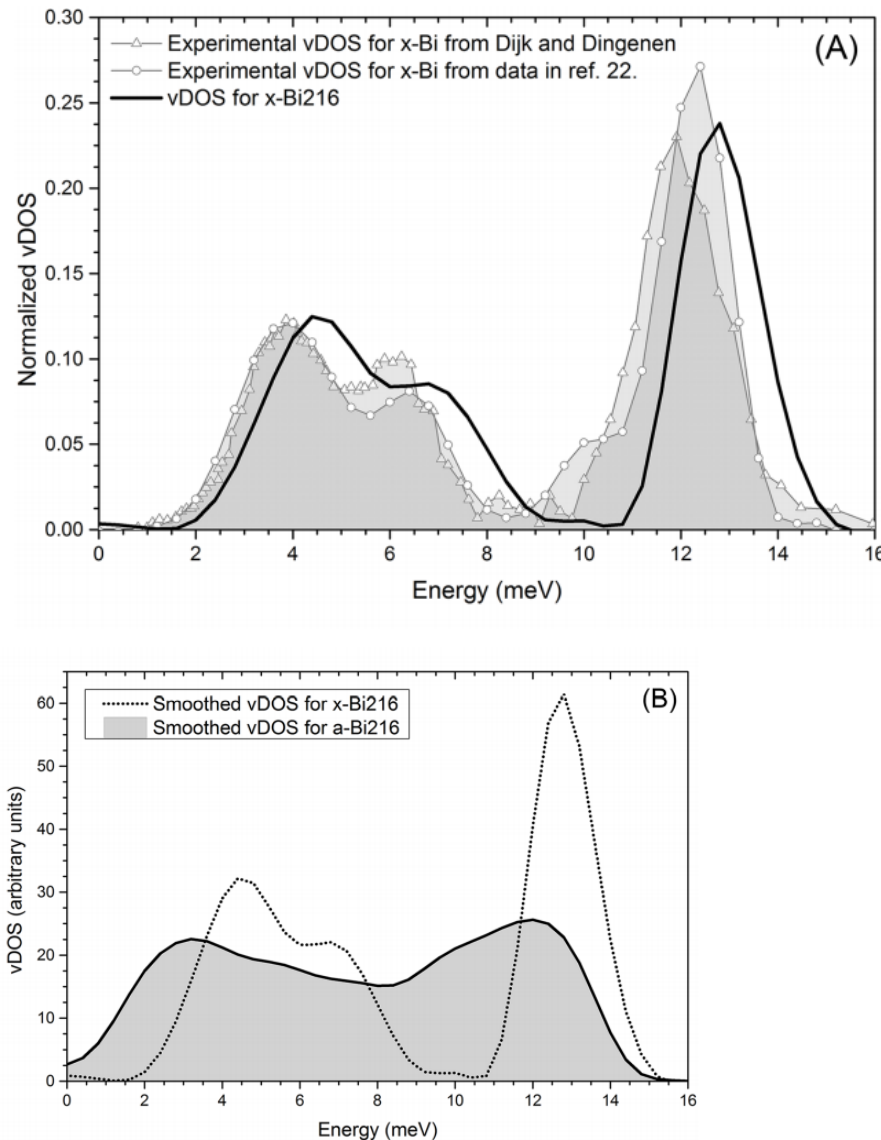


**Fig 5. Vibrational behavior for the crystalline and the amorphous.** (A) Comparison of the experimental vDOS (extracted and processed from Kakizaki [31] and taken from the results of Dijk and Dingenen [20]) and our computational calculations for x-Bi. The curves have been normalized so that the area under each curve is 1. (B) Comparison of the calculated vDOS for crystalline and amorphous supercells x-Bi216 and a-Bi216. The area under each curve has been set equal to  $3N_A$ .

---

## Superconductivity in Bismuth

An approach to superconductivity can be done using simple **BCS** approach or **McMillan** approach, which is more complete and involves more **parameters ad-hoc**.

We first present a simple BCS estimate of a possible crystalline superconducting transition temperature:

- **A la BCS:** The attractive interaction between electrons via **phonons (e-ph)** is fundamentally important for the occurrence of superconductivity and is related to the **factor  $V$**  in the BCS equation for the **critical superconducting transition temperature  $T_c$** . In the original form of the BCS theory  $T_c$  can be evaluated by

$$T_c = 1.13\theta_D \exp \left[ -\frac{1}{N(E_F)V} \right] \quad (1)$$

Where  $N(E_F)$  is the electronic density of states at the Fermi level ( $E_F$ ) and  $V$  is the e-ph coupling potential.

In equation (1) we take  $\theta_D = \hbar\omega_D/k_B$ . With  $\omega_D$  given by (**Debye things**):

$$\omega_D = \exp \left[ 1/3 + \frac{\int_0^{\omega_{max}} \log(\omega) F(\omega) d\omega}{\int_0^{\omega_{max}} F(\omega) d\omega} \right] \quad (2)$$

This equation is assumed valid for  $T \geq \theta_D$ . The value of  $\omega_D$  in equation 2 is an upper limit to the real value of the **Debye frequency**.

$\omega_D$  is calculated using eq 2 and our simulational results for  $F(\omega)$ .

We obtain a value of  $\theta_D$  of 100K for amorphous and 129K for crystalline.

These results are pretty similar to experiment.

Using eq 1 and assuming  $T_c^c$  is the transition temperature for crystalline and  $T_c^a$  is for amorphous.

We can calculate the value for x-Bi to be  $T_c^c = 1.3mK$ . This result is smaller than the  $50mK$  reported experimentally for amorphous.

But assuming that the e-ph interaction for amorphous and crystalline are the same is a strong assumption.

- **A la McMillan:** Assuming that x-Bi may be described by McMillan's formula, we calculate the corresponding parameters to obtain an estimation of the electron phonon interaction, or equivalently, of the strength of the parameter  $\lambda$ .

An experimental result for  $\lambda$  for a-Bi using tunneling experiments leads to  $\lambda^a = 2.46$ . The parameter  $\lambda$  can be calculated in terms of  $\alpha^2(\omega)$  and  $F^c(\omega)$  as follows:

$$\lambda^c = 2 \int_0^\infty \omega^{-1} \alpha^2(\omega) F^c(\omega) d\omega$$

The result is  $\lambda^c = 0.98$ .

This implies that if, in fact, the value of  $\lambda^c$  is less than 1, then x-Bi should be in the **weak coupling regime** if it is a superconductor.

This corroborates the assumption of the preponderance of the e-e attraction in the amorphous with respect to the crystalline.

The relationship among  $T_c$ ,  $\theta_D$ ,  $\mu^*$  and  $\lambda$  in the McMillan formalism is given by

$$T_c = \frac{\theta_D}{1.45} \exp \left[ \frac{-1.04(1+\lambda)}{(\lambda - \mu^*(1+0.62\lambda))} \right]$$

Where  $\mu^*$  is the **Coulomb pseudopotential**

A plot of  $T_c(\lambda)$  vs  $\lambda$  appears in Fig 6, where the value of  $\mu^* = 0.105$  is used. This shows that the  $T_c$  dependence on  $\lambda$  is not very strong for high values of  $\lambda$ . For low values,  $T_c$  changes rapidly with  $\lambda$ .

For the superconducting transition temperature estimated in the BCS formalism, 1.3 mK, the  $\lambda$  obtained is 0.236.

This indicates that the e-ph coupling is much stronger in the a-Bi than in x-Bi, 2.46 vs 0.236. So the coupling constant for amorphous is more than 11 times as intense as for crystalline.

So the assumption of the similarity of the strength of the electron phonon interaction in both x-Bi and a-Bi used earlier should be handled with care, and the estimated transition temperature of 1.3mK should be considered an upper limit for the crystalline material.

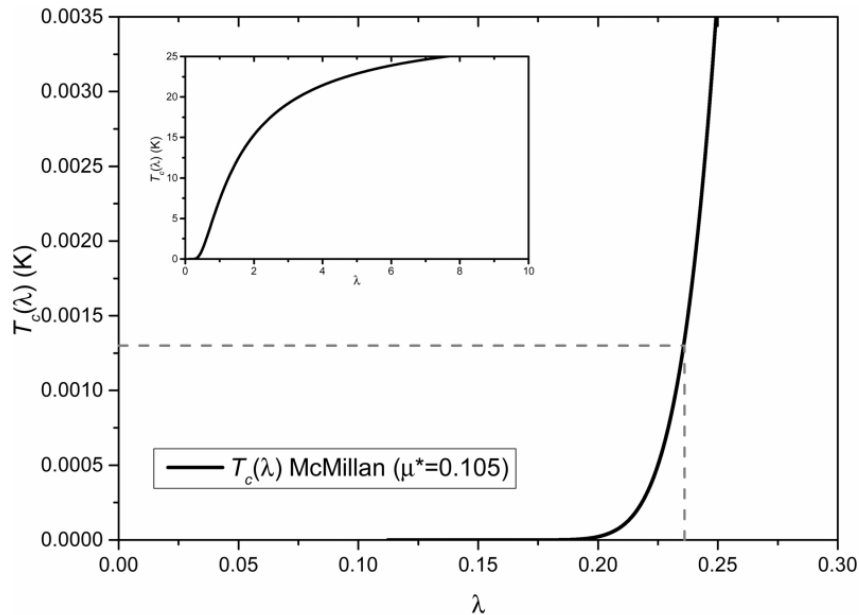


**Fig 6. Dependence of  $T_c(\lambda)$  on  $\lambda$  from McMillan's Eq.4 for  $\theta_D = 129K$ .** The behavior indicates that the  $T_c$  dependence on  $\lambda$  is not very strong for high values of  $\lambda$ . For low values,  $T_c$  changes rapidly with  $\lambda$ . The inset is an extended plot. The dotted lines show the value of  $\lambda$  (0.236) for the estimated  $T_c$ .

doi:10.1371/journal.pone.0147645.g006

---

## Specific Annotations

### The structure Simulations

#### The modified undermelt-quench process

To generate the structure of a-Bi we start with a 216 atom **diamond like supercell** with an edge length of 19.7 Å and periodic boundary conditions, a-Bi216.

Since x-Bi has a rhombohedral structure, the diamond-like structure is unstable and will disorder readily as the temperature is raised.

At temperatures just below the melting point, the structure becomes non-crystalline, but upon cooling has the tendency to crystallize so the time step has to be chosen adequately to avoid this change of phase.

We chose interatomic distances on the initial structure that are close to the real bond lengths and a density close to the solid crystalline bismuth.

The computational procedure is performed with the code **FASTSTRUCTURE** that uses the **Local Density Approximation (LDA)** to perform **DFT**.

to solve the interactions in the system a linear combination of atomic orbitals **LCAO** is used, so a set of basis functions are needed; the **Vosko Wilk and Nusair (VWN)**. The cutoff of the orbital functions is set to 5Å, to just include second neighbors.

The computational process to amorphize structures is called the **undermelt quench**.

Originally the process consisted first of heating the supercell to just below the melt cooling the system down to close to 0 K (quench), and finally using a set of thermal panels to relax the stresses that appear in the sample.

This method was originally applied successfully to semiconductors, so we had to change it. The initial supercell is heated from 300 K to 540 K (4.5 K below the bismuth melting point) in 100 computational steps. Then it is quenched from 540 K to close to 0 K in 225 steps to maintain the same absolute thermal rate for the heating and the cooling processes.

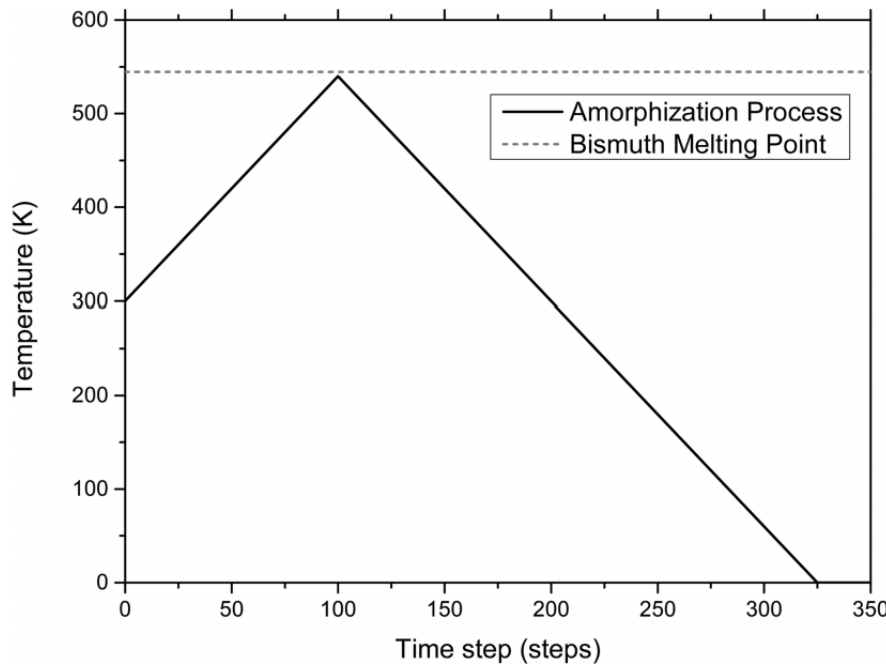


Fig 7. The modified *undermelt-quench* process. This is the amorphization process used to generate amorphous bismuth supercells. The heating ramp stops just below the melting point whereas the cooling ramp has the same (negative) slope.

Once the processes are finished, a **geometry optimization** is performed to guarantee that the energy of the structure is a minimum, representing a metastable amorphous solid. In all cases periodic boundary conditions are incorporated.

After obtaining the structure, the **PDF** can be calculated from the atomic positions. But since the number of atoms is small, the PDF is smoothed to emulate a large number of atoms. This done with a **2 point fast Fourier smoothing**. The smoothing weight is chosen so as the peaks of the calculation have the same height as those of the experimental PDF.

## Electronic and Vibrational Simulations

In order to obtain the eDOS from the final amorphous structure, we perform a single-point energy calculation using the DMol3 code with finer parameters than for the structural calculations. For these calculations, the **Density-functional Semi core Pseudo Potential (DSPP)** approximation is used. The electronic calculations were performed at the supercell **Gamma point** since no symmetries were involved. We compare the experimental vDOS for x-bi with the one calculated.

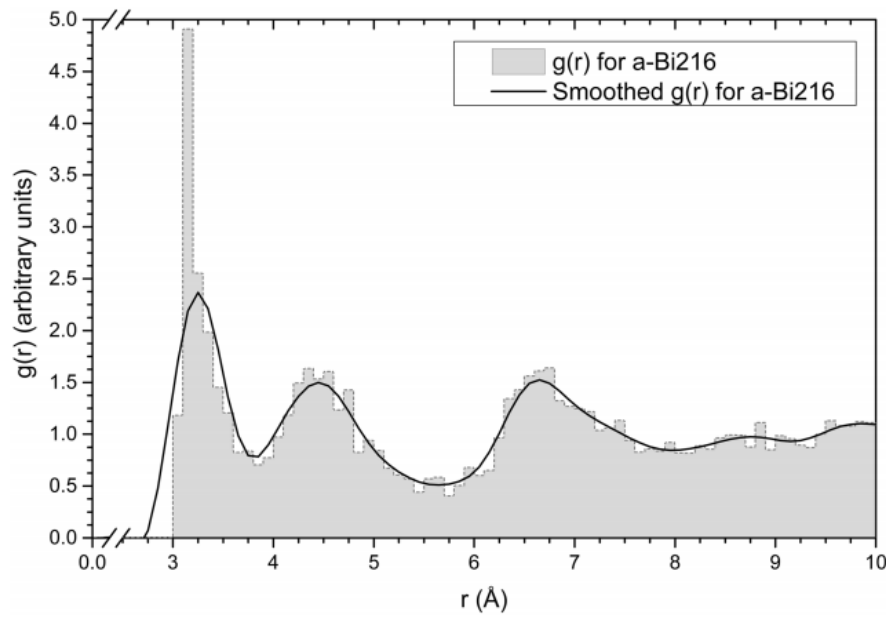


**Fig 8. The amorphous PDF (or  $g(r)$ ).** The figure shows the amorphous  $g(r)$  (grey filled figure) and its 2-point smoothed curve (continuous black line) for a-Bi<sub>216</sub>.

---

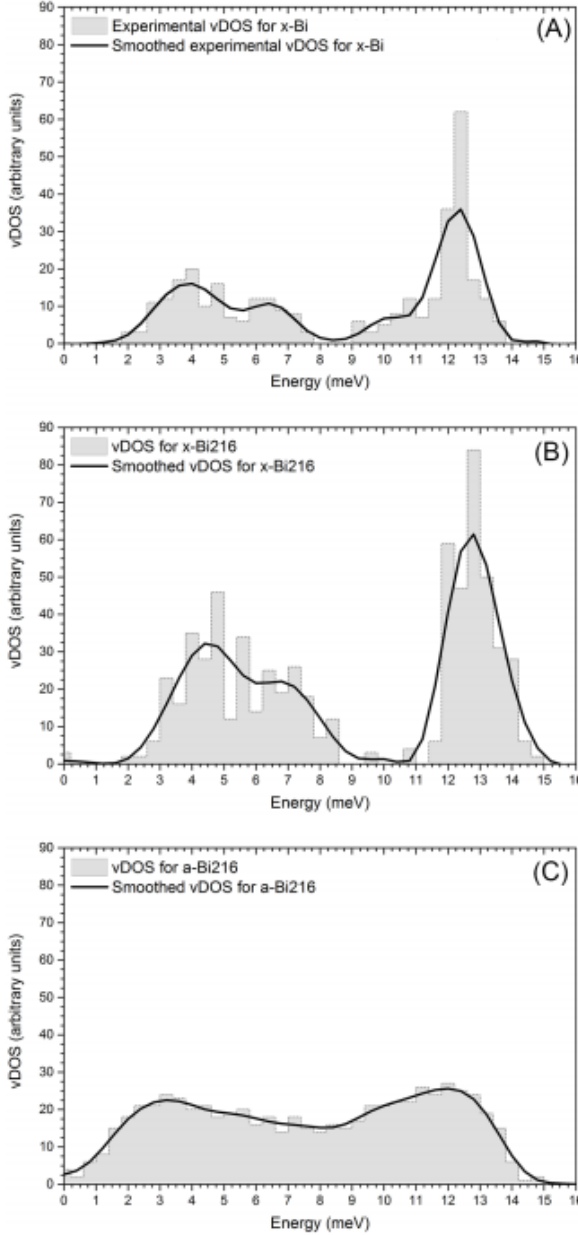


**Fig 9. The vibrational distributions vDOS (or  $F(\omega)$ ).** The figures show the vDOS (grey filled figures) and their 3-point smooth curves (continuous black lines) for (A) the experimental x-Bi (10) (B) the theoretical x-Bi216 calculated in this work and (C) the theoretical a-Bi216 calculated in this work.

We digitize the experimental phonon dispersion curves and apply a frequency count with a bin of width of  $0.4\text{meV}$ . Then applying a **3 point FF smoothing** on this data and normalize the smoothed curve to 3 times the number of atoms. The same procedure is applied to the data obtained from the frequency calculations done on the a-Bi216 supercell.

## A simple Superconductivity analysis

We assume that bismuth is a **BCS** superconductor and we incorporate the changes in the eDOS at the **Fermi level**  $N(E_F)$  in going from crystal to amorphous.

---

Assuming that superconductivity is possible for x-Bi, with a **superconducting transition temperature**  $T_c^c$  and that  $V$  is essentially the same for the amorphous and crystalline phases, we can then estimate  $T_c^c$  in terms of  $T_c^a$  as follows.

The BCS equation for the crystalline material is:

$$T_c^c = 1.13\theta_D^c \exp[-1/N^c(E_F)V^c]$$

And for the amorphous phase the equation becomes:

$$\begin{aligned} T_c^a &= 1.13\theta_D^a \exp[-1/4N^a(E_F)V^a] \\ (T_c^a)^4 &= (1.13\theta_D^a)^4 (\exp[-1/4N^a(E_F)V^a])^4 \end{aligned}$$

Since  $4N^c(E_F) \simeq N^a(E_F)$ . Taking the ratio  $T_c^c/(T_c^a)^4$ , we obtain:

$$\frac{T_c^c}{(T_c^a)^4} = \frac{1.13\theta_D^c}{(1.13\theta_D^a)^4}$$

And if we accept that  $1.3\theta_D \simeq \theta_D^c$  as calculated in this work, this becomes:

$$R_c^c = \frac{1.3(T_c^a)^4}{(1.13\theta_D^a)^3}$$

Since  $T_c^a$  is  $6.2K$ , the experimental result, gives a crystalline transition temperature of  $T_c^c = 1.32 \times 10^{-3}K$

## Conclusions

We report the computer generation of amorphous bismuth that displays pair distribution functions for a 216-atom supercell in agreement with experiment. Assuming this agreement is an indication of the representativeness of our amorphous structure, we then proceed to calculate the electronic and vibrational densities of states for both amorphous and crystalline supercells.

These results suggest that the marked differences found are responsible for the radically different superconducting properties. Estimations of a transition temperature for the crystalline, assuming that the relevant factors are the eDOS and vDOS leads us to predict an upper bound for the superconducting transition temperature of the order of 1.3 mK.

Features to be noted are that the electronic density of states of the amorphous is about 4 times larger than the crystalline at the Fermi level, and that the vibrational density of states of the amorphous develops a noticeable accumulation of phonon modes at low frequencies along with the disappearance of the “gap” at intermediate frequencies.

---

## Artículo 2

### Possible superconductivity in Bismuth (111) bilayers. Their electronic and vibrational properties from first principles

David Hinojosa-Romero<sup>1</sup>, Isaías Rodríguez<sup>2</sup>, Alexander Valladares<sup>2</sup>, Renela M. Valladares<sup>2</sup> and Ariel A. Valladares<sup>1 \*</sup>.

<sup>1</sup>*Instituto de Investigaciones en Materiales, Universidad Nacional Autónoma de México, Apartado Postal 70-360, Ciudad Universitaria, CDMX, 04510, México.*

<sup>2</sup>*Facultad de Ciencias, Universidad Nacional Autónoma de México, Apartado Postal 70-542, Ciudad Universitaria, CDMX, 04510, México*

### Abstract

We use a 72 atom **supercell** to report **ab initio** calculations of the **electronic and vibrational densities of states** for the **bismuth (111) bilayers (bismuthene)** with **periodic boundary conditions** and a **vacuum** of 5A, 10A and 20A.

We find that the electronic density of states of states shows a **metallic character** at the **Fermi level**. And that the vibrational density of states manifests the **expected gap** due to the **layers**.

Our results indicate that a vacuum down to 5A does not affect the electronic and vibrational structures noticeably.

A comparison of present results with those obtained for the **Wyckoff structure** is displayed. Assuming that the **Cooper pairing potential** is similar for all phases and structures of bismuth, an estimate of the superconducting transition temperature gives 2.61K for the bismuth biayers.

### Introduction

**Bulk Bismuth** is known to be a **semimetal**, a **metal** or a **superconductor**. With peculiar electronic and vibrational properties depending on whether it is **crystalline** or **amorphous** or depending on the pressure.

At ambient pressure and temperature, it crystallizes in the **Wyckoff structure**, *Bi-I* with **rhombohedral symmetry** in which each atom has 3 equidistant nearest neighbor atoms and 3 equidistant next nearest neighbors slightly further away. Resulting in a **buckled 2D honeycomb bilayer** lying perpendicular to the [111] **crystallographic direction**.

---

**Bismuthene**, or the **bilayers (111) of bismuth**, **Bi(111)**, recently has been subject to investigation as an example of low dimensional materials and the influence of this in electronic ant transport properties.

It has been argued that in this layered form, bismuth has properties of **topological insulators** [2-4] which are **bulk insulators** with **protected boundary states**.

This state of matter appears when there is an **inversion in the electronic bands** of **2D materials** caused by perturbations. Among the perturbing agents, there is **strains in the systems, controlled quantum well width, doping**.

We claim that *Bi(111)* bilayers may display superconductivity at liquid helium temperatures. The original **BCS** explanation of superconductivity introduced two concepts:

- **Phonon mediated electron Cooper pairing** due to vibrations in the material.
- **Coherent motion** of the paired electrons that gives them the inertia to sustain electrical currents.

We here show that summoning the corresponding electron and vibrational densities of states of a given structure, superconductivity may appear provided the Cooper attraction sets in. This, if proven correct, would indicate that superconductivity in bismuth can be understood in a simple manner without invoking eccentric mechanisms.

We recently demonstrated that the Wyckoff crystalline phase of Bi may become superconducting (artículo 1). This phase had been investigated for decades with no superconductivity found. However, after our publication, an experimental group investigated it at temperatures lower than the upper bound we calculated ( $T_c \leq 1.3mK$ ), and found that this phase is indeed superconducting at  $T_c = 0.53mK$

We have shown that a simple compression without allowing for changes in crystalline structures cannot predict the appearance of superconductivity of the phases of Bi under pressure. If modifications in the crystalline structures are permitted, then the eDOS and vDOS will change and we consider that these are the factors that explain superconductivity in the different phases and structures of bismuth.

## Method

We calculate and analyze the  $N(E)$  and  $F(\omega)$  for the Wyckoff and bismuthene structures looking for a justification to validate that Bi (111) bilayers become a superconductor.

We estimate the transition **a la Mata Pinzón et al** (artículo anterior).

We proceed using a **supercell** with 240 atoms. For bismuthene we use a **slab model** which consists of a 72 atom supercell with 5A, 10A and 20A of **vacuum spacing** between Bismuth (111) bilayers including **periodic boundary conditions**.

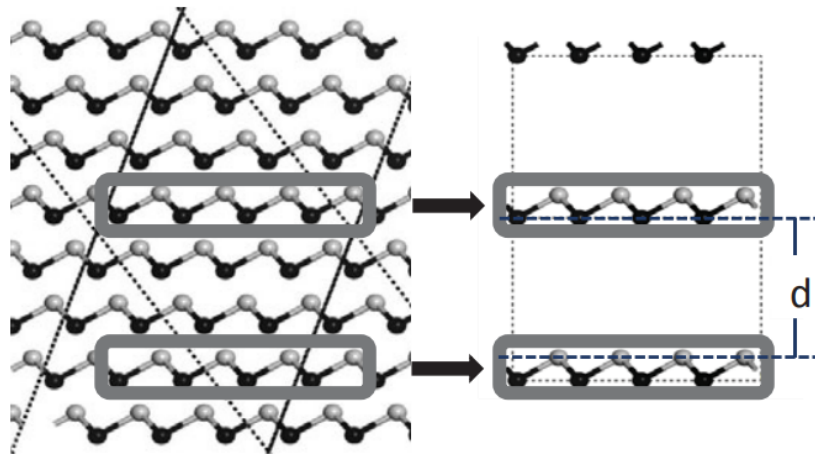


**Figure 1.** Construction of the supercell for Bi (111). Starting with the Wyckoff structure (left) we consider two identical slabs separated by a distance  $d$  (right). The bilayer is set to lie on the  $xy$  plane of the new supercell.

$N(E)$  and  $F(\omega)$  are calculated using the DMol3 code which is part of the Materials Studio suite.

To obtain the eDoS, a single point energy calculation was performed using a **double numeric(dn) basis set** and a **fine mesh** within the **LDA-VWN** approximation. An unrestricted spin-polarized calculation for the energy was carried out.

Since bismuth is a heavy element with many electrons, the **density functional semi core pseudo potential (DSPP)** approximation was used. DSPPs have been designed to generate accurate DMol3 calculations, so we expect a good approximation.

The parameters used in the calculations were the same for  $N(E)$  and  $F(\omega)$ , so meaningful comparisons can be made.

We now base our discussion on the **BCS** expression for the transition temperature:

$$T_c = 1.13\Theta_D \exp[-1/(N(E_F)V_0)]$$

Where  $\theta_D$  is the **Debye temperature** and represents the role played by the vibrational density of states vDoS typified by  $F(\omega)$ .

$N(E_f)$  is the eDoS at the **Fermi level**  $E_F$

$V$  is the **Cooper pairing potential** that binds pairs of electrons.

Here we can see a graph of this, for some specific arbitrary value of  $V$ , to see the strong dependence on  $N(E_F)$

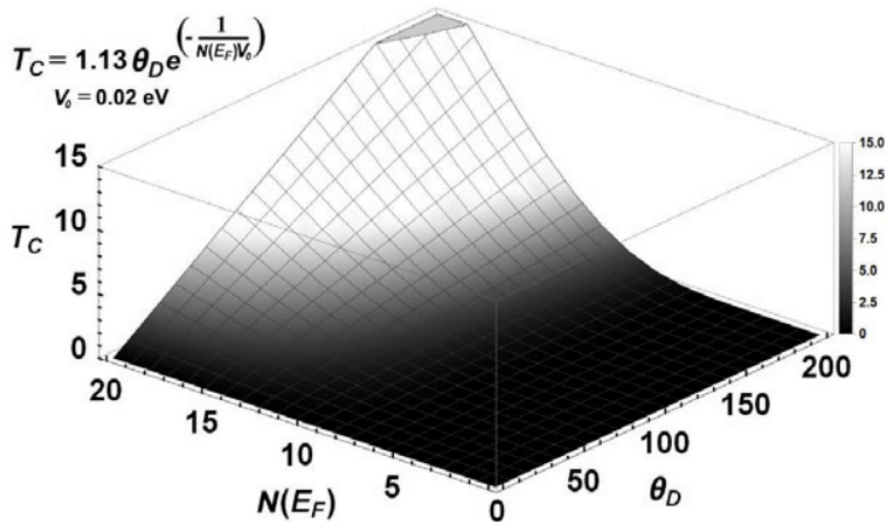


**Figure 2.** Dependence of the superconducting transition temperature  $T_c$  on the electronic  $N(E_F)$  and vibrational  $\theta_D$  parameters. The pairing potential  $V_0 = 0.02$  eV was chosen arbitrarily.

This shows that under certain circumstances,  $N(E_F)$  can play a more important role than the vibrations. Especially when different geometries of the same material are compared since in this case it can be assumed that the strength of the pairing potential would not be altered much by these changes. Although the Debye temperatures may not change drastically, the electronic properties could change radically going from being bulk to becoming a bismuthene, case at hand.

## Results and Discussion

For the eDoS the DMol3 analysis tools included in the Materials Studio suite were used, set to eV, and also an integration method with a smearing width of 0.2 eV. The number of points per eV was 100. The results for the densities of states are given per atom in Figure 3,  $N(E)/\text{atom}$ .

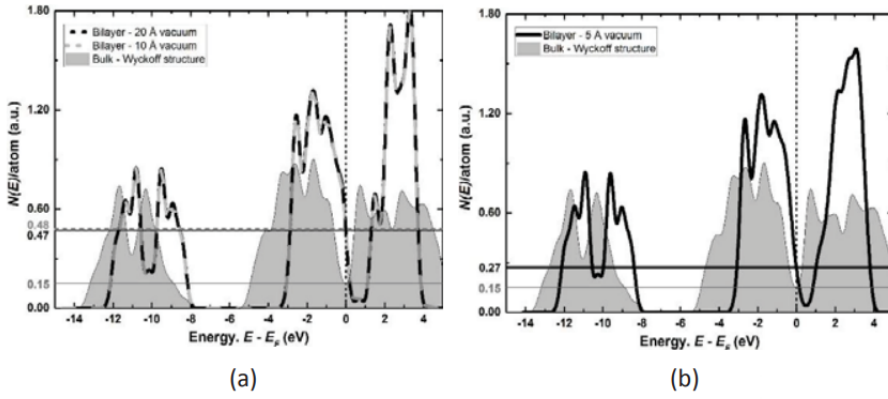


**Figure 3.** Comparison of the electron densities of states for the Wyckoff (shaded plot) and Bi (111) structures. (a) The eDoS for the layers  $N(E)^L$  are practically the same for  $d= 10 \text{ \AA}$  and  $20 \text{ \AA}$ , dashed lines. (b) When  $d= 5 \text{ \AA}$   $N(E)^L$  changes drastically at  $E_F$ , solid line. The vertical axis is  $N(E)/\text{atom}$  so that we can compare supercells of different sizes.  $E_F$ , the Fermi energy, is the reference value for the energy.

For the vDoS the results were analyzed with Origin Pro. The normal modes calculated were imported in **THz**. A frequency count with 0.11 THz bin width was used, and the resulting bins were smoothed using a **two point FFT filter**. We give the results of  $F(\omega)/\text{atom}$ .

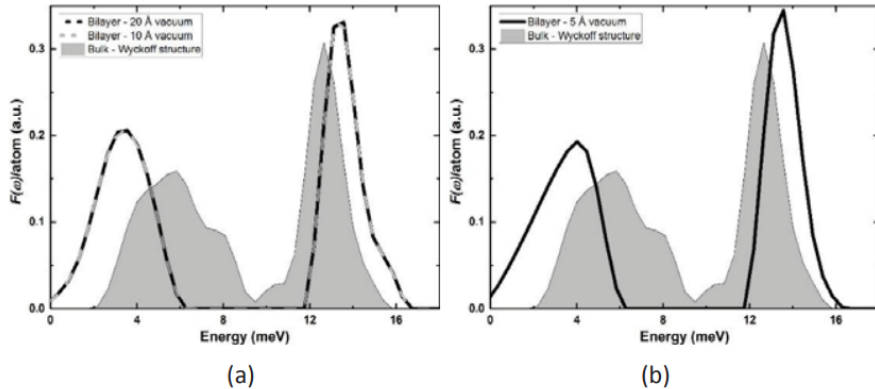


**Figure 4.** Comparison of the vibrational densities of states for the Wyckoff (shaded plot) and Bi (111) structures. (a) The vDoS for the layers  $F(\omega)^L$  are practically the same for  $d= 10 \text{ \AA}$  and  $20 \text{ \AA}$ , dashed lines. (b) When  $d= 5 \text{ \AA}$  there are some minor changes in  $F(\omega)^L$ , solid line. The vertical axis is  $F(\omega)/\text{atom}$  so that we can compare supercells of different sizes.

In figure 3a) the values of Bi(111) of  $N(E)^L$ , the eDoS for the layered structures for  $d = 10\text{\AA}$  and  $20\text{\AA}$  are compared to the Wyckoff  $N(E)^W$  result.

The  $N(E)^L$  has a higher number of electron state, 0.48 at the Fermi level, indicating a **metallic character**.  $N(E)^W$  as expected is lower in comparison, since this phase is semimetallic, 0.15. The ratio of the densities of electron states at the Fermi level is 3.20.

To incorporate the **Debye temperatures** as required by eq 1, we need to calculate them from the vibrational spectra presented in Figures 4. For this we use an expression due to

---

Grimvall:

$$\omega_D = \exp \left[ 1/3 + \frac{\int_0^{\omega_{\max}} \log(\omega) F(\omega) d\omega}{\int_0^{\omega_{\max}} F(\omega) d\omega} \right]$$

and  $\Theta_D = \hbar\omega_D/k_B$

$F(\omega)$  is the vDoS of the supercell.

$\omega_{\max}$  is the maximum frequency of the **vibrational spectrum**.

We also use the second expression and find that

- $\Theta_D^L = 104.3K$
- $\Theta_D^W = 134.2K$

The ratio being of 0.78

To obtain these results, we removed the **translational modes**  $\omega \simeq 0$  that are more preponderant the smaller the number of atoms in a supercell.

The experimental values for  $\theta_D$  reported by DeSorbo [20] for crystalline bismuth at ambient pressure varies from 140 K at high temperatures to 120 K at low temperatures. Our calculations indicate that  $\theta_D$  for the crystal at ambient pressure lies between the experimental values so we trust the results of 134.2 K for Wyckoff and 104.3 K for Bi (111).

Now we may compare the possible  $T_c$  for the *Bi(111)* structure with the  $T_c^W$  of the Wyckoff phase.

We do it with the superconductivity we predicted for the Wyckoff phase in the BCS approach. Suppose that superconductivity is possible for *Bi(111)*, with a superconducting transition temperature  $T_c^L$ , and assume the **Cooper pair potential**  $V$  is essentially the same for these two structures of the material. Then the transition temperatures are:

$$T_c^L = 1.13\Theta_D^L \exp[-1/(N(E_F)^L V_0)]$$

$$T_c^W = 1.13\Theta_D^W \exp[-1/(N(E_F)^W V_0)]$$

If we assume that  $N(E_F)^L = \alpha N(E_F)^W$  and  $\Theta_D^L = \beta \Theta_D^W$ , we can find that:

$$T_c^L = \{T_c^W\}^{1/\alpha} \beta (1.13\Theta_D^W)^{(\alpha-1)/\alpha}$$

We substitute the values  $\alpha = 3.2$  and  $\beta = 0.78$  and the superconducting temperature of W structure to find:

$$T_c^L = 2.61K$$

---

## Conclusions

The bilayers of bismuth, bismuthene are very interesting because they form the basic structure of bulk bismuth, and they may display interesting properties when isolated. That is why we have investigated their electronic and vibrational properties as a function of the interlayer separation.

We find that for interlayer distances higher than or equal to  $d = 5 \text{ \AA}$  the properties of the layers are practically identical, which means that the interaction between them is practically negligible.

As the layers approach one another, the properties will resemble those of bulk bismuth although to obtain the Wyckoff phase a translation has to occur when interlayer distances approach the bulk ones.

Assuming that the Cooper pairing potential remains unchanged in going from bulk to layer, we predict, based on the changes in the eDoS of these structures that the layer will superconduct at  $T_c^L = 2.61K$

---

## Artículo 3

### *Ab initio Study of the Amorphous Cu-Bi System*

D. Hinojosa-Romero<sup>1</sup>, I. Rodriguez<sup>2</sup>, A. Valladares<sup>2</sup>, R. M. Valladares<sup>2</sup>, A. A. Valladares<sup>1\*</sup>

*1 Condensed Matter Department, Instituto de Investigaciones en Materiales, UNAM.*

*2 Physics Department, Facultad de Ciencias, UNAM.*

\* Corresponding Author: Ariel A. Valladares, valladar@unam.mx

### Abstract

As a pure element, bismuth is a semimetal with many interesting properties. The recent discovery of superconductivity, as predicted by our group, and the increasing superconducting transition temperature as the pressure applied increases, are some examples of its particularities.

Also, the fact that the amorphous phase is superconductive with a transition temperature several orders of magnitude larger than the crystalline at ambient pressure is unusual. These phenomena have motivated our predictions for the transition temperatures of Bi-bilayers and the Bi-IV phase.

When mixed with other elements, bismuth seems to contribute to the superconducting character of the resulting material. Here we study the binary copper-bismuth amorphous system which is known to superconduct in diverse compositions.

Using **ab initio molecular dynamics** and the **undermelt quench method**, we generate an **amorphous structure** for a 144 atom supercell corresponding to the  $Cu_{61}Bi_{39}$  system.

We calculate the electronic and vibrational densities of states for the amorphous system and estimate a superconducting critical temperature of  $4.2K$  for the amorphous state.

### Introduction

Along the years, several theories explaining the superconducting behavior of solids have emerged, each one proposing different mechanisms in which the pairing of electrons occur. However, the successful predictions of the BCS theory remain up to present time.

According to BCS theory, the fundamental properties that determine the  $T_c$  for a particular solid are the **density of electronic states at the Fermi level**  $N(E_F)$ , the **Debye temperature**  $\theta_D$  and the **electron phonon coupling** represented through the **interaction potential**  $V_0$ .

This is expressed in the equation:

$$T_c = 1.13\theta_D \exp(-1/N(E_F)V_0)$$

which is plotted in the Figure for  $V_0 = 0.02\text{ eV}$  and reflects the fact that  $T_c$  is more sensitive to  $N(E_F)$  than to  $\theta_D$

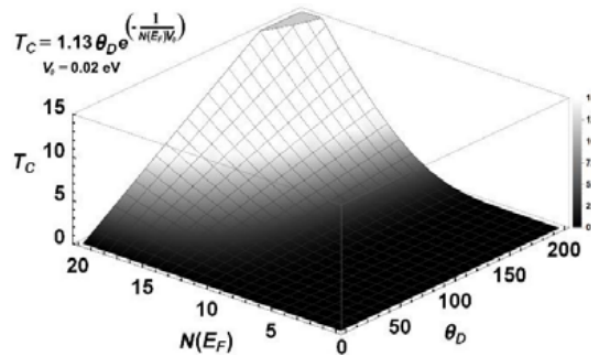


Figure 1. The BCS theory predicts a transition temperature that depends on the vibrational properties  $\theta_D$  and the electronic properties  $N(E_F)$ .  $V_0$  was chosen as 0.02 for our purposes.

By means of first principles calculations and equation (1), our group predicted the  $T_c$  for the bismuth crystalline system at atmospheric pressure (artículo 1), which was later experimentally verified. Also, we have performed calculations for Bi-bilayer systems (artículo 2) and the Bi-IV phase under-pressure, both awaiting experimental validation.

Following this line of investigation, in this work we expand our study to bismuth compounds, particularly the Cu-Bi system which is known to superconduct in the amorphous structure, possessing a  $T_c$  ranging from 1 to 6 K depending on the composition

In order to assess the effect of structural disorder in this system, we studied and compared the amorphous with the recently obtained crystalline structure using highpressure synthesis of the Cu<sub>61</sub>Bi<sub>39</sub> system, as reported by S. Clarke et al. who measured a  $T_c$  of 1.36 K for this crystalline phase.

## Methodology

For the study of the crystalline structure of Clarke, we constructed a 144-atom supercell with the same crystalline structure reported by them. That is 88 copper atoms and 56 Bismuth arranged in a **monoclinic structure** with space group  $C2/m$  and density of  $10.29\text{ g/cm}^3$

---

For the generation of amorphous structure, we constructed a 144 atom supercell with an ordered unstable FCC structure and the same density and composition of its crystalline counterpart.

Then we performed an **undermelt-quench** approach, linearly heating it from 300 K to 1080 K and then rapidly cooling to 8K. The resulting structure was then optimized and we calculated the PDF.

We then calculated the eDOS for the crystalline  $N^c(E)$  and for amorphous  $N^a(E)$  structures. We also obtained the **vDOS** from which we get the **Debye temperatures**  $\theta_D^c$  and  $\theta_D^a$  using:

$$\omega_D = \exp[1/3 + (\int \log(\omega)F(\omega)d\omega / \int F(\omega)d\omega)]$$

Assuming that the potential  $V_0$  doesn't change between both structures (crys and amor) and considering the **amorphous to crystallin ration**  $\eta$  of the **electronic states at the Fermi level**. And the **Debye tmpерatures ratio**  $\delta$ . We estimated the superconducting transition temperature for the amorphous system  $T_c^a$ , a la Mata et al:

$$T_c^a = \delta(1.13\theta_D^c)^{(\eta-1)/\eta}(T_c^C)^{1/\eta}$$

In which the measured critical temperature  $T_c^C$  and the calculated Debye temperature  $\theta_D^c$  for the crystalline structure have been taken as reference.

All calculations were performed using the DFT approach implemented in the DMOL3 with the following parameters:

- **dnd basis**
- **unrestricted spin polarization**
- *dspp* pseudopotential with the *VWN* functional
- **real space cut off radius** of 5A for both elements
- A 2x2x1 **k-poin mesh**

## Results

The optimized structured of the amorphous system  $a - Cu_{61}Bi_{39}$  is shown in a ball model. The **parameters of the supercell** are  $a = b = 12.79A, c = 17.06A$  and  $\alpha = \beta = \gamma = 90^\circ$ . Resulting in a density of  $10.29g/cm^3$

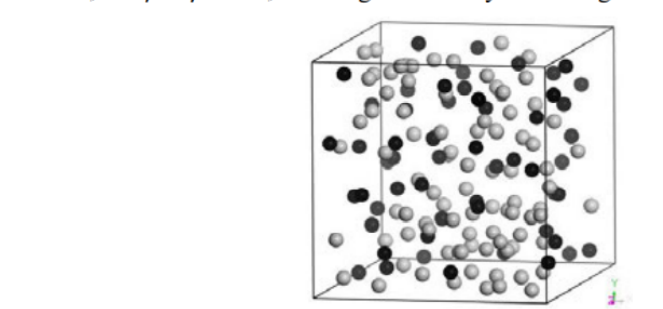


Figure 2. Ball model of the resulting optimized amorphous structure of the Cu<sub>61</sub>Bi<sub>39</sub> system. Grey spheres represent copper atoms and black spheres represent bismuth atoms.

The **total and weighted partial PDFs** for the amorphous structure are shown. There are remnants of a **second peak bimodality** (characteristic of amorphous metallic systems, as can be seen in *Cu – Cu* partial PDF around 4 to 5 Å).

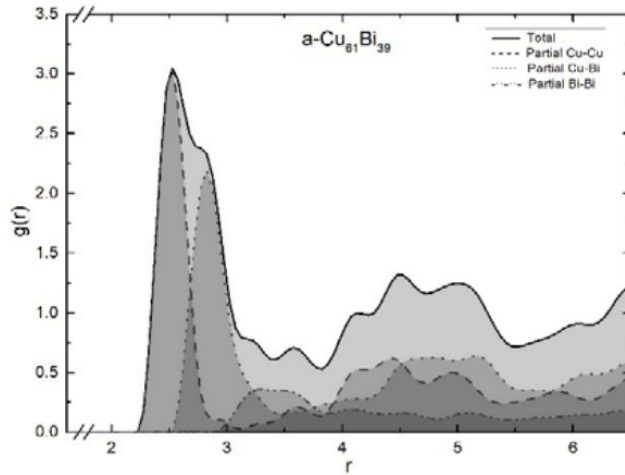


Figure 3. Total (solid) and weighted-partial (dashed, Cu-Cu; dotted, Cu-Bi; dash-dotted Bi-Bi) PDFs for the a-Cu<sub>61</sub>Bi<sub>39</sub> system.

The eDoS per atom for a-Cu<sub>61</sub>Bi<sub>39</sub> and crystalline c-Cu<sub>61</sub>Bi<sub>39</sub> are shown. The general shape is the same for both.

However, the ratio amorphous to crystalline for the number of states at the Fermi level  $\eta$  is 1.27, propitiating important changes on the electronic properties for the mixture, such as the superconducting transition temperature as we shall see.

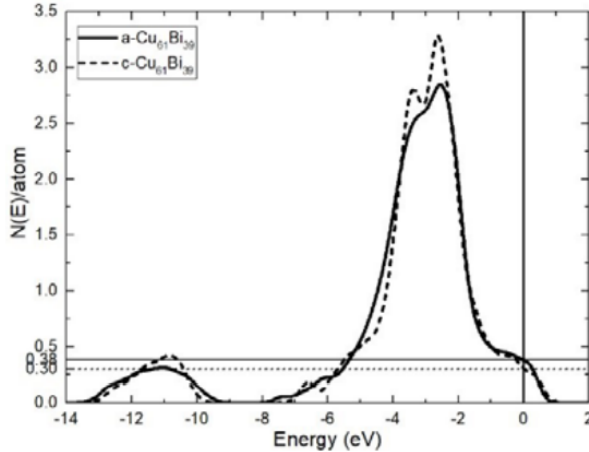


Figure 4. Comparison of the eDoS per atom for the crystalline (dashed) and amorphous (solid) structures.  $N(E_F)/\text{atom}$  is 0.30 and 0.38 for the respective structures.

Now we obtain the **vibrational modes** for a and c. They were smoothed with a 3-point FFT, we get:

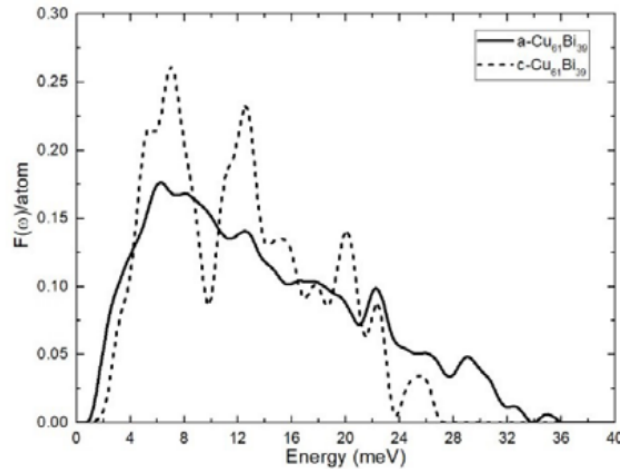


Figure 5. Comparison of the vDoS per atom for the crystalline (dashed) and amorphous (solid) structures. The three translational modes were removed from the graph.

Using  $F(\omega)$ , we calculated the  $\theta_D$  to be 182.62K for amorphous and 170.07K for the crystalline. So we have  $\delta = 1.07$

Then using equation(2), we calculate  $T_c$  for amorphous and get 4.2K

## Conclusion

We obtained an amorphous sample for the Cu61Bi39 system by means of ab initio molecular dynamics and the undermelt quench approach. Resulting in a structure with a PDF that resembles the typical shape for amorphous metallic materials.

---

The eDOS doesn't differ significantly in amorphous and crystalline. In contrast, the vDOS of both are different.

The analysis leads to a transition temperature of 4.2 K.

---

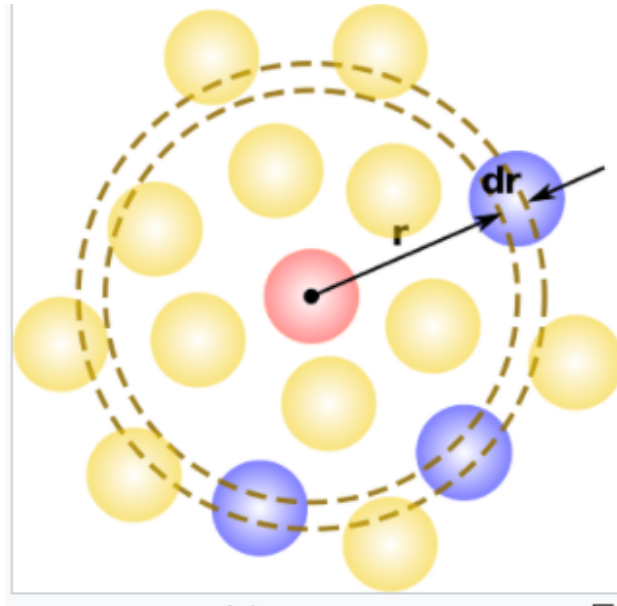
## Glosario y Cosas

- **Bismuth:** Is a chemical element with atomic number 83. The electron configuration is  $4f^{14}5d^{10}6s^26p^3$ . The electrons per shell are 2, 8, 18, 32, 18, 5. It has a density of  $9.78g/cm^3$  and a melting point of  $544.7K$ . No other metal is verified to be more naturally diamagnetic than bismuth. Of any metal, it has the lowest values of thermal conductivity and it has a high electrical resistivity.
- **Amorphous Solid:** It is a solid that lacks long range order. It is a non crystalline solid.
- **Crystalline Solid:** A solid whose constituents are arranged in a highly ordered microscopic structure, forming a crystal lattice that extends in all directions. Crystalline solids have atoms in a near perfect periodic arrangement.
- **Pair distribution function:** It is a function that describes the distribution of distances between pairs of particles contained within a given volume. If  $a$  and  $b$  are two particles in a fluid, the pair distribution of  $b$  with respect to  $a$ , denoted by  $g_{ab}(\vec{r})$  is the probability of finding the particle  $b$  a distance  $\vec{r}$  from  $a$ , with  $a$  the origin of coordinates.

The **Radial distribution function**  $g(r)$  is a measure of the probability of finding a particle at a distance of  $r$  away from a given reference particle, relative for that for an ideal gas.

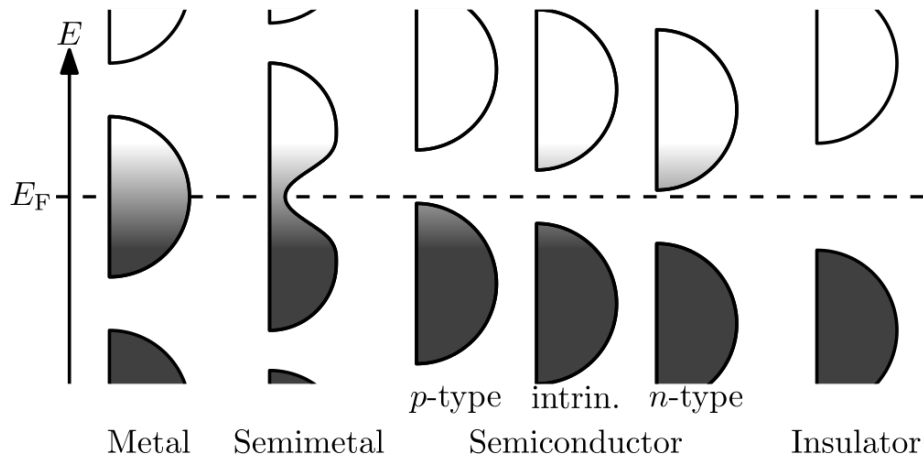
The algorithm involves determining how many particles are within a distance of  $r$  and  $r + dr$  away from a particle.

This is determined by calculating the distance between all particle pairs and binning them into a histogram. The histogram is then normalized with respect to an ideal gas. For 3D, this normalization is the number density of the system  $\rho$  multiplied by the volume of the spherical shell, which is  $\rho 4\pi r^2 dr$



- **Undermelt Quench:** It is the method to obtain an amorphous structure of a solid. We begin with the crystalline structure (I think) and we heat it until a temperature just below the melting temperature. Then, we cool it with steps of the same size until we get to a temperature close to 0K. Then, we perform geometry optimization and get the amorphous solid.
- **Geometry Optimization:** It is the process of changing the system's geometry (nuclear coordinates and potentially the lattice vectors) to minimize the total energy of the systems. The optimization is usually local, it converges to the next local minimum on the potential energy surface.
- **Electronic Density of States (eDOS):** The density of states describes the proportion of states that are to be occupied by the system at each energy. It is defined as  $D(E) = N(E)/V$  where  $N(E)\delta E$  is the number of states in the system of volume  $V$  whose energies lie in the range from  $E$  to  $E + \delta E$ . In is mathematically represented as a distribution by a probability density function.

In QM particles can occupy modes or states with wavelengths dictated by the system, often only specific states are permitted. It can happen that many states are available for occupation at a specific energy level, while no states are available at other energy levels.



**Vibrational Density of States (VDOS):** Also called phonon density of states. It is the density of vibrational states depending on energy.

**Fermi Energy:** It refers to the energy difference between the highest and the lowest occupied single particle states in a quantum system of non interacting electrons (only defined at absolute 0). It is the energy of the highest energy level and can only be defined for non interacting fermions.

To find the ground state of a whole system of fermions, we start with an empty system and add particles one at a time, consecutively filling up the unoccupied stationary states with lowest energy. When the particles have been put in, the Fermi energy is the kinetic energy of the highest occupied state (remember it is at 0K).

The Fermi energy of a non interacting ensemble of identical spin 1/2 fermions in a 3D system is given by  $E_F = \frac{\hbar^2}{2m_0} \left( \frac{3\pi^2 N}{V} \right)^{2/3}$

**Fermi Level:** It is the thermodynamic work required to add one electron to the body.

**BCS theory:** A theory that describes superconductivity.

At low temperatures, electrons near the Fermi surface become unstable against the formation of **Cooper pairs** (pairs of electrons that are slightly bound together due to phonon-electron interactions). The e-ph interaction makes a paired electron state have a lower energy than the Fermi energy, so it is preferable.

Given the e-e attraction, the Cooper pairs have now bosonic properties, so at sufficiently low temperatures, they form Bose-Einstein condensates.

This condensates have the effect of giving the body 0 resistance.

**Superconducting Transition Temperature:** It is the temperature below which a material superconducts.

**Phonon:** A phonon is a collective excitation in a periodic arrangement of atoms in condensed matters. They can be thought of as quantized sound waves.

---

**e-ph interaction:** An electron in a conductor will attract nearby positive charges in the lattice. This deformation of the lattice (phonon) causes another electron, with opposite spin to be attracted to this zone.

**McMillan's formula:** It is a formula used to find the transition temperature of a material

$$T_c = 1.13\theta_D \exp\left[-\frac{1}{N(E_F)V}\right]$$

- **Debye Model:** It is a method developed by Debye for estimating the phonon contribution to specific heat in a solid. It treats the vibrations of the atomic lattice (heat) as phonons in a box. It correctly predicts the low temperature dependence of the heat capacity, which is proportional to  $T^3$ , the **Debye  $T^3$  law**. It also recovers the **Dulong Petit law** at high temperatures, but suffers at intermediate.

**Debye frequency:**  $\omega_D$ : Is a parameter in the Debye model. It refers to a cut off angular frequency for waves of a harmonic chain of masses.

**Debye temperature:**  $\theta_D$ : It is the temperature of a crystal's highest normal mode of vibration. i.e the highest temperature that can be achieved due to a single normal vibration. They are related by:

$$\theta_D = \frac{\hbar}{k_B} \omega_D$$

**Metastable state:** Excited state that is stable but isn't the lowest state. So a little push won't disturb this metastable state, but a big one will probably take it to a lower energy. That is, it is a local but not global minimum of energy.

- **Coordination number:** The number of nearest neighbors to an atom in a solid.
- **Ab initio:** From the beginning, from first principles.
- **DFT:** It is a computational QM modelling method used in materials science to investigate the electronic structure (or nuclear structure) principally in the ground state. DFT calculations allow the prediction and calculation of material behavior on the basis of quantum mechanical considerations, without requiring higher-order parameters such as fundamental material properties.

In contemporary DFT techniques the electronic structure is evaluated using a potential acting on the system's electrons. This DFT potential is constructed as the sum of

external potentials  $V_{ext}$ , which is determined solely by the structure and the elemental composition of the system, and an effective potential  $V_{eff}$ , which represents interelectronic interactions. Thus, a problem for a representative supercell of a material with  $n$  electrons can be studied as a set of  $n$  one-electron Schrödinger-like equations, which are also known as Kohn–Sham equations.

**Kohn Sham equations:** It is the one electron Schrodinger equation of a fictitious system of non interacting particles that generate the same density as the system of interacting ones.

**Electron Density:** A measure of the probability of an electron being present at an infinitesimal element of space around any given point.

### Hohenberg-Kohn theorems:

- **Theorem 1:** The external potential is a unique functional of the electron density
- **Theorem 2:** The functional that delivers the ground state energy of the system gives the lowest energy iff the input density is the true ground state density.

## Teoría de funcionales de la densidad

- Para el estado base reducimos el problema de  $3N$  variables a solo 3:

$$E[\Psi(\vec{r}_1, \vec{r}_2, \dots, \vec{r}_N)] = E[\rho(\vec{r})]$$

- Ecuaciones de Kohn-Sham:

$$V_{eff}^{KS}(\vec{r}) = V_{ext}(\vec{r}) + \frac{e^2}{4\pi\epsilon_0} \int \frac{\rho_e(\vec{r}')}{|\vec{r} - \vec{r}'|} d^3\vec{r}' + V_{xc}(\vec{r})$$

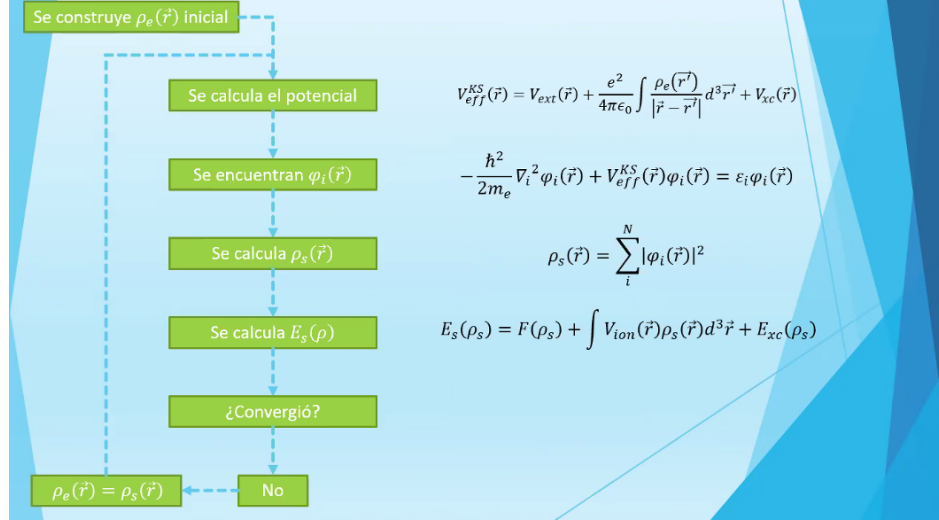
$$-\frac{\hbar^2}{2m_e} \nabla_i^2 \varphi_i(\vec{r}) + V_{eff}^{KS}(\vec{r}) \varphi_i(\vec{r}) = \varepsilon_i \varphi_i(\vec{r})$$

$$\rho_s(\vec{r}) = \sum_i^N |\varphi_i(\vec{r})|^2$$

$$E_s(\rho_s) = F(\rho_s) + \int V_{ion}(\vec{r}) \rho_s(\vec{r}) d^3\vec{r} + E_{xc}(\rho_s)$$

# Teoría de funcionales de la densidad

## Ciclo auto consistente (Self-Consistent Field)



**Annealing:** In metallurgy, annealing is a heat treatment that alters the physical and sometimes chemical properties of a material. It involves heating a material above its recrystallization temperature, maintaining a suitable temperature for an appropriate amount of time and then cooling.

- **Harris Functional:** In density functional theory (DFT), the Harris energy functional is a non-self-consistent approximation to the Kohn–Sham density functional theory.[1] It gives the energy of a combined system as a function of the electronic densities of the isolated parts. The energy of the Harris functional varies much less than the energy of the Kohn–Sham functional as the density moves away from the converged density.
- **LDA:** Local-density approximations (LDA) are a class of approximations to the exchange–correlation (XC) energy functional in density functional theory (DFT) that depend solely upon the value of the electronic density at each point in space (and not, for example, derivatives of the density or the Kohn–Sham orbitals). Many approaches can yield local approximations to the XC energy. However, overwhelmingly successful local approximations are those that have been derived from the homogeneous electron gas (HEG) model. In this regard, LDA is generally synonymous with functionals based on the HEG approximation, which are then applied to realistic systems (molecules and solids).

**DMOL:** DMol3 is a commercial (and academic) software package which uses density functional theory with a numerical radial function[1] basis set to calculate the electronic properties of molecules, clusters, surfaces and crystalline solid materials [2] from

---

first principles.

- **Periodic Boundary Conditions:** Periodic boundary condition (PBCs) are a set of boundary conditions which are often chosen for approximating a large (infinite) system by using a small part called a unit cell. PBCs are often used in computer simulations and mathematical models.
- **Single point energy calculations:** A single point energy (SPE) calculation calculates the wavefunction and charge density, and hence the energy, of a particular (arbitrary) arrangement of nuclei.
- **PAD (Plane angle distribution):** Probability distribution of finding another particles depending on the angle.
- **3 point Fast Fourier Filter:** Using a Fast fourier to smooth out a graph

- **Angle Resolved photoemission spectroscopy:** Angle-resolved photoemission spectroscopy (ARPES) is an experimental technique used in condensed matter physics to probe the allowed energies and momenta of the electrons in a material, usually a crystalline solid.

Electrons in crystalline solids can only populate states of certain energies and momenta, others being forbidden by quantum mechanics. They form a continuum of states known as the band structure of the solid. The band structure determines if a material is an insulator, a semiconductor, or a metal, how it conducts electricity and in which directions it conducts best, or how it behaves in a magnetic field.

Angle-resolved photoemission spectroscopy determines the band structure and helps understand the scattering processes and interactions of electrons with other constituents of a material. It does so by observing the electrons ejected by photons from their initial energy and momentum state into the state whose energy is by the energy of the photon higher than the initial energy, and higher than the binding energy of the electron in the solid.

**Semimetal:** A semimetal is a material with a very small overlap between the bottom of the conduction band and the top of the valence band.